Statistical Analysis of Quantum Annealing

Xinyu Song[1], Yazhen Wang[2], Shang Wu[2] Donggyu Kim[3],

[1] School of Statistics and Management,
Shanghai University of Finance and Economics
[2] Department of Statistics,
University of Wisconsin-Madison
[3] College of Business,
Korea Advanced Institute of Science and Technology

March 1, 2022

Abstract

Quantum computers use quantum resources to carry out computational tasks and may outperform classical computers in solving certain computational problems. Special-purpose quantum computers such as quantum annealers employ quantum adiabatic theorem to solve combinatorial optimization problems. In this paper, we compare classical annealings such as simulated annealing and quantum annealings that are done by the D-Wave machines both theoretically and numerically. We show that if the classical and quantum annealing are characterized by equivalent Ising models, then solving an optimization problem, i.e., finding the minimal energy of each Ising model, by the two annealing procedures, are mathematically identical. For quantum annealing, we also derive the probability lower-bound on successfully solving an optimization problem by measuring the system at the end of the annealing procedure. Moreover, we present the Markov chain Monte Carlo (MCMC) method to realize quantum annealing by classical computers and investigate its statistical properties. In the numerical section, we discuss the discrepancies between the MCMC based annealing approaches and the quantum annealing approach in solving optimization problems.

Keywords and phrases: Combinatorial optimization, ground state success probability, Hamiltonian, Ising model, Markov chain Monte Carlo (MCMC), quantum computing, quantum annealing

Running title: Quantum Annealing and MCMC

1 Introduction

While classical computation follows classical physics and uses electronic transistors to crunch zeros and ones individually, quantum computation employs quantum resources to manage zeros and ones simultaneously and may speed up certain calculation work dramatically (Nielsen and Chuang, 2000; Wang, 2012). Quantum computation strives to understand how to take advantage of the huge information hidden in quantum systems by exploring the enormous potential of atoms and photons. It uses quantum phenomena such as quantum superposition, quantum entanglement and quantum tunneling to compute and process infomation. Two major approaches to realize and implement quantum computation are logic-gate based quantum computing and adiabatic quantum computing (Aharonov et al., 2008; Browne, 2014; Deutsch, 1985; DiVincenzo, 1995; Farhi et al., 2000, 2001, 2002; Johnson et al., 2011). The logic-gate based quantum computers are constructed based on quantum circuits with quantum gates and provide the quantum analog of classical universal or general-purpose computers. Intensive efforts are underway around the world by academic labs, large companies, and government institutes to overcome technical problems in constructing the universal quantum computers. However, the practical application of general-purpose quantum computers may be still decades away while on the other hand, special-purpose quantum computers such as quantum annealers and quantum simulators, can be constructed with capabilities exceeding their classical counterparts (Aharonov and Ta-Shma, 2003; Aharonov et al., 2008; Albash and Lidar, 2016; Britton et al., 2012; Browne, 2014; Brumfiel, 2012; Wang, 2012). Quantum annealers are physical hardwares to realize quantum annealing and are used to solve combinatorial optimization problems and to realize Monte Carlo sampling more efficiently. Annealing materials by first heating and then slow cooling in order to reduce their brittleness is an ancient technology, which has been used in making and refining materials such as glass and metal. Computers can be employed to reproduce this process, which creates simulated annealing that provides an optimization tool. It is based on the analogy between the behavior of a complex physical system with multiple degrees of freedom and an optimization problem of finding the global minimum given an objective function defined by many parameters. The objective function of the optimization problem can be regarded as the energy of the physical system, then finding the minimum energy configurations or ground states of the many-body physical system is equivalent to solving the corresponding optimization problem. Computer simulation algorithms can be developed to mimic the annealing procedure of the physical system and finally reach the minimum energy configurations. We discuss the classical approach called simulated annealing (SA) and the quantum approach called quantum annealing.

Given an optimization problem, SA takes into account the relative configuration energies and a fictitious time-dependent temperature when exploring the immense search space probabilistically. Specifically, we assign the physical system a temperature that can be regarded as a control parameter introduced artificially. By slowly driving the temperature from a high value to zero, we are able to move the physical system to the state with the lowest value of energy, hence also arrive at the solution of the optimization problem (Bertsimas and Tsitsiklis, 1993; Kirkpatrick et al., 1983; Wang et al., 2016). Quantum annealing con-

structs on the physical process of a quantum system whose lowest energy or equivalently, the ground state of the system, represents the solution to an optimization problem posed. It first establishes a simple quantum system initialized in its ground state, and then gradually moves the simple system to the target complex system. Quantum adiabatic theorem (Farhi et al., 2000, 2001, 2002; Kadowaki and Nishimori, 1998) indicates that the system will likely to stay in the ground state during the gradual evolution, thus, under certain probability, we can find the solution of the original optimization problem by measuring the system at its final state. That is, quantum annealing replaces thermal fluctuations in SA by quantum tunneling to keep the system close to its instantaneous ground state during the evolution. It is similar to a quasi-equilibrium state being maintained during the evolution of SA. See Brooke et al. (1999); Isakov et al. (2016); Jörg et al. (2010); Wang et al. (2016) for more details. Both the classical and quantum annealing methods are powerful tools for solving hard optimization problems, whether achieved by physical devices or simulation methods. The physical scheme either employs a natural system or builds a device to engineer a physical system where the ground state of the system represents the sought-after solution of an optimization problem (McGeoch, 2014). The simulation approach applies "escape" rules in computer simulations to prevent the system from getting trapped in local minima given a cost function, and eventually, reach the global minimum with some probability (Martoňák et al., 2002; Rieger and Kawashima, 1999). In both situations, the system can probabilistically explore its the huge configuration space, and finally freeze in the global minimum with certain probability. Through sufficient repeated attempts, we can find the global minimum and solve the optimization problem.

Quantum annealing devices are actively pursued by several academic labs and companies such as Google and D-Wave Systems, with uncertain quantum speedup. For example, the D-Wave quantum computer is a commercially available hardware device that is designed and built to implement quantum annealing physically. It is an analog computing device based on superconducting quantum bits (also called qubits) to process the annealing procedure and solve combinatorial optimization problems (Albash et al., 2015; Boixo et al., 2014, 2016, 2018; Brady and van Dam, 2016; Rønnow et al., 2014; Wang et al., 2016). The D-Wave computers have been used to solve simple optimization problems in graphs and networks, machine learning, artificial intelligence, and computational biology (Bian et al., 2013; O'Gorman et al., 2015; Perdomo-Ortiz et al., 2012, 2015; Rieffel et al., 2015). As an example, the lowest energy alignment of a protein is considered as its preferred state, and protein folding is to find the lowest energy point in its energy landscape; the D-Wave computers can be arranged to manipulate qubits to reach their lowest energy state and solve the folding problem of a simple protein (McGeoch, 2014; Perdomo-Ortiz et al., 2012).

The rest of the paper proceeds as follows. Section 2 briefly reviews quantum mechanics and quantum computation. Section 3 introduces quantum annealing and discusses its implementations by the D-Wave devices and its realizations by the MCMC based methods, called simulated quantum annealing (SQA), in the contex of Ising model. Section 4 carries out simulation experiments by classical computers to illustrate SA and SQA. The results are compared with ground state success probability data obtained from quantum annealing. Section 5 features concluding remarks regarding statistical issues associated with the study

of the D-Wave devices and whether those MCMC based annealing methods can provide statistical models for the D-Wave devices.

2 A brief quantum background

2.1 Notations

For this paper, we consider the finite dimension only and let $\mathbb{C}^d$ be the d-dimensional complex space. For a vector ψ in $\mathbb{C}^d$, we employ the usual notations in quantum science and use Dirac notations ket $|\cdot\rangle$ and bra $\langle\cdot|$ to denote the column $|\psi\rangle$ and row $\langle\psi|$ vector. Let the superscripts $*$, $\prime$ and $\dagger$ be the conjugate of a complex number, the transpose of a vector or matrix, and the conjugate transpose operation, respectively. A natural inner product in $\mathbb{C}^d$ is given by $\langle u|v\rangle = \sum_{j=1}^{d} u_j^* v_j = (u_1^*, \cdots, u_d^*)(v_1, \cdots, v_d)'$, where $\langle u| = (u_1, \cdots, u_d)$ and $|v\rangle = (v_1, \cdots, v_d)'$, and the modulus follows to be $|u| = \sqrt{\langle u|u\rangle}$. A matrix $\mathbf{A}$ is said to be Hermitian if $\mathbf{A} = \mathbf{A}^\dagger$ and a matrix $\mathbf{U}$ is said to be unitary if $\mathbf{U}\mathbf{U}^\dagger = \mathbf{U}^\dagger\mathbf{U} = \mathbf{I}$, where $\mathbf{I}$ is an identity matrix.

2.2 Qubit and superposition

In classical computation, the most fundamental entity is a bit with two mutually exclusive state values 0 and 1. The quantum analog of the classical bit is a qubit with two state values $|0\rangle$ and $|1\rangle$, where we use the customary notation $|\cdot\rangle$ called ket to denote the qubit state. Moreover, quantum computation allows qubits to encode the two states, zeros and ones, simultaneously, which is known as the quantum superposition. That is, a qubit can be in superposition states $|\psi\rangle = \alpha_0|0\rangle + \alpha_1|1\rangle$ where complex numbers α_0 and α_1 are called amplitudes and satisfy $|\alpha_0|^2 + |\alpha_1|^2 = 1$. Thus, the states of a qubit are unit vectors in $\mathbb{C}^2$, and the states $|0\rangle$ and $|1\rangle$ form an orthonormal basis for the $\mathbb{C}^2$ space, which are known as computational basis states. Unlike the classical bits that have mutually exclusive states and can be examined to determine whether it is in state 0 or 1, the qubits can be zero and one simultaneously while its state cannot be determined by examing the qubit. Instead, by quantum mechanics, we can measure a qubit $|\psi\rangle$ and obtain either the result 0, with probability $|\alpha_0|^2$, or the result 1, with probability $|\alpha_1|^2$.

Like classic bits, we also can define multiple qubits. For one b-qubit, its states are unit vectors in a 2^b-dimensional complex vector space with computational basis states of the form $|x_1x_2\cdots x_b\rangle$, $x_j = 0$ or 1, $j = 1, \ldots, b$. For example, the states of 2-qubit are unit vectors in $\mathbb{C}^4$ space with the superposition states $|\psi\rangle = \alpha_{00}\,|00\rangle + \alpha_{01}\,|01\rangle + \alpha_{10}\,|10\rangle + \alpha_{11}\,|11\rangle$, where amplitudes α_x are complex numbers satisfying $|\alpha_{00}|^2 + |\alpha_{01}|^2 + |\alpha_{10}|^2 + |\alpha_{11}|^2 = 1$. Similar to the single qubit case, we obtain a measurement outcome x as one of the $00, 01, 10, 11$ with a corresponding probability $|\alpha_x^2|$. The quantum exponential complexity is then shown in the exponential growth of dimensionality 2^b and the number of 2^b amplitudes needed to specify the superposition states. Thus, as the quantum systems evolves, they are able to store and keep track an exponential number of complex numbers while performing data manipulations

and calculations. See Nielsen and Chuang (2000) and Wang (2012) for details.

2.3 Quantum physics

Quantum systems are entirely characterized by their states and the time evolution of the states. For a fixed time, the states of a d-dimensional quantum system can be characterized by a unit vector $|\psi\rangle$ in $\mathbb{C}^d$. To study the quantum system, we perform measurements on an observable $\mathbf{M}$, which is a Hermitian matrix on $\mathbb{C}^d$. The eigendecomposition of $\mathbf{M}$ is assumed to be the following

$$\mathbf{M} = \sum_{a=1}^{r} \lambda_a \mathbf{Q}_a,$$

where $\lambda_1, \ldots, \lambda_r$ are the real eigenvalues of $\mathbf{M}$, and $\mathbf{Q}_a$ is the projection onto the eigen-space corresponding to the eigenvalue λ_a. Quantum probability theory says that if we measure $\mathbf{M}$ for the quantum system under the state $|\psi\rangle$, we may obtain the measurement outcome Λ, which is a random variable that takes values in $\{\lambda_1, \lambda_2, \ldots, \lambda_r\}$ with probability distribution $P(\Lambda = \lambda_a) = \mathrm{tr}(\mathbf{Q}_a|\psi\rangle\langle\psi|) = \langle\psi|\mathbf{Q}_a|\psi\rangle$, $a = 1, 2, \ldots, r$. Statistically, we can measure $\mathbf{M}$ many times to obtain measurement data for making inferences on the quantum states.

We now focus on the time evolution of a quantum system. Let $|\psi(t)\rangle$ be the state of the quantum system at time t, which is known as a wave function. The states $|\psi(t_1)\rangle$ and $|\psi(t_2)\rangle$ at times t_1 and t_2 are connected through $|\psi(t_2)\rangle = \mathbf{U}(t_1, t_2)\,|\psi(t_1)\rangle$, where $\mathbf{U}(t_1, t_2) = \exp[-i\,\mathbf{H}\,(t_2 - t_1)]$ is a unitary matrix and $\mathbf{H}$ is a Hermitian matrix on $\mathbb{C}^d$. In this regard, the continuous time evolution of $|\psi(t)\rangle$ is governed by the following Schrödinger equation

$$\sqrt{-1}\,\frac{\partial|\psi(t)\rangle}{\partial t} = \mathbf{H}|\psi(t)\rangle \;\text{ or equivalently }\; |\psi(t)\rangle = e^{-\sqrt{-1}\,\mathbf{H}t}|\psi(0)\rangle, \tag{2.1}$$

here $\mathbf{H}$ is a possibly time-dependent Hermitian matrix on $\mathbb{C}^d$, which is known as the Hamiltonian of the quantum system for governing its quantum evolution. See Cai et al. (2016); Holevo (2011); Sakurai and Napolitano (2017); Shankar (2012); Wang (2012, 2013) and Wang and Xu (2015) for details.

3 Quantum annealing and MCMC simulations

In this section, we first review the classical simulated annealing and then discuss the quantum annealing. We show that if the simulated and quantum annealing are described by equivalent Ising models, then solving the corresponding optimization problem, or equivalently, finding the minimal energy of each Ising model, are mathematically identical by the two annealing approaches. We also derive the ground state success probability for quantum annealing and present the path-integral Monte Carlo method to mimic the quantum annealing by classical simulation. Relevant statistical theorems are presented.

3.1 Simulated annealing

Ising model is often used to describe the natural systems in physics and many optimization problems can be mapped into physical systems described by the Ising model. Examples include traveling salesman problem, portfolio optimization, integer factoring, social economics network, protein folding, protein modeling, and statistical genetics. The ground state of the Ising model provides a solution for the optimization problem (Irbäck et al., 1996; Majewski et al., 2001; McGeoch, 2014; Stauffer, 2008).

Ising model is described by a graph $\mathcal{G} = (\mathcal{V}(\mathcal{G}), \mathcal{E}(\mathcal{G}))$, where $\mathcal{V}(\mathcal{G})$ and $\mathcal{E}(\mathcal{G})$ represent the vertex and edge sets of $\mathcal{G}$, respectively. Each vertex is occupied by a random variable whose value is $\{+1, -1\}$, and each edge corresponds to the coupling (or interaction) between two vertex variables connected by the edge. A configuration $\mathbf{s} = \{s_j, j \in \mathcal{V}(\mathcal{G})\}$ is defined as a set of values assigned to all vertex variables s_j, $j \in \mathcal{V}(\mathcal{G})$. We refer to the vertices as sites and vertex variables as spins in physics, where $+1$ is for spin up and -1 is for spin down. As a case in point, consider a graph corresponding to a 2-dimensional lattice with a magnet placed at each lattice site facing either up or down. Given b lattice sites and at each site j, we let the variable s_j be a binary random variable representing the position of the magnet, where $s_j = \pm 1$ can be interpreted as the jth magnet pointing up or down, respectively.

The classical Ising model has the following Hamiltonian

$$\mathbf{H}_I^c(\mathbf{s}) = -\sum_{(i,j)\in\mathcal{E}(\mathcal{G})} J_{ij} s_i s_j - \sum_{j\in\mathcal{V}(\mathcal{G})} h_j s_j, \tag{3.2}$$

where (i, j) stands for the edge between the sites i and j, the first sum takes over all pairs of vertices with edge $(i, j) \in \mathcal{E}(\mathcal{G})$, J_{ij} stands for the interaction (or coupling) between sites i and j associated with edge $(i, j) \in \mathcal{E}(\mathcal{G})$, and h_j describes an external magnetic field on vertex $j \in \mathcal{V}(\mathcal{G})$. We refer to a set of fixed values $\{J_{ij}, h_j\}$ as one instance of the Ising model. Given a specific configuration $\mathbf{s}$, the energy of the Ising model is $\mathbf{H}_I^c(\mathbf{s})$.

According to Boltzmann's law, the probability of a given configuration $\mathbf{s}$ is described by the following Boltzmann (or Gibbs) distribution

$$P_\beta(\mathbf{s}) = \frac{e^{-\beta \mathbf{H}_I^c(\mathbf{s})}}{Z_\beta}, \qquad Z_\beta = \sum_{\mathbf{s}} e^{-\beta \mathbf{H}_I^c(\mathbf{s})}, \tag{3.3}$$

here $\beta = (k_B T)^{-1}$ is an inverse temperature where k_B a generic physical constant called the Boltzmann constant and T the absolute temperature, moreover, the normalization constant Z_β is called the partition function. If $k_B = 1$, then T serves as the fundamental temperature of the system with units of energy, and β is reciprocal to the fundamental temperature. The configuration probability $P_\beta(\mathbf{s})$ denotes the probability that the physical system is in a state with configuration $\mathbf{s}$ in equilibrium.

When using the Ising model to represent a combinatorial optimization problem, the goal is to find the ground state of the Ising model, that is, we need to find a configuration that can minimize the energy function $\mathbf{H}_I^c(\mathbf{s})$. If the Ising model contains b sites, then the configuration space is $\{-1, +1\}^b$ and the total number of possible configurations is 2^b. We note that

the system complexity increases exponentially in the number of sites b, and thus, it is very difficult to find the ground states and solve the minimization problem numerically when b is large. In fact, the search space that grows exponentially prohibits us to solve the minimization problem with deterministic exhaustive search algorithms. Instead, annealing methods such as SA can be employed to search the space probabilistically. To find the configuration with minimal energy, SA uses MCMC methods such as Metropolitan Hastings algorithm to generate configuration samples from the Boltzmann distribution while decreasing the temperature slowly. We initialize the algorithm with a random spin configuration and flip spins at each step randomly. A new spin configuration is accepted if it lowers the energy and if not, it is accepted probabilistically based on the Metropolis rule; meanwhile, the temperature is lowered to reduce the escape probability of trapping in local minima. That is, the initial spin configuration $\mathbf{s}^{(0)} = \{s_j^{(0)}\}$ is obtained by randomly and independently assign $+1$ or -1 to each spin. The spins are updated in sequence, and one sweep means a complete updating over all spins. At the kth sweep, we attempt to flip the ith spin from state $s_i^{(k-1)}$ to the new state $s_i^{(k)} = -s_i^{(k-1)}$ while all the other spins remain unchanged. The change of energy caused by the flipping is the following

$$\Delta E_i^{(k)} = -h_i(s_i^{(k)} - s_i^{(k-1)}) - \sum_{j=1}^{i-1} J_{ij} s_j^{(k)}(s_i^{(k)} - s_i^{(k-1)}) - \sum_{j=i+1}^{b} J_{ij} s_j^{(k-1)}(s_i^{(k)} - s_i^{(k-1)}).$$

The state of the ith spin is updated from $s_i^{(k-1)}$ to $s_i^{(k)}$ if the energy is lowered, that is, $\Delta E_i^{(k)} \leq 0$; otherwise, the state is updated with probability $\exp(-\Delta E_i^{(k)}/T_k)$, where T_k is the annealing schedule to lower the temperature. That is, the new state $s_i^{(k)}$ is accepted with probability $\min\{1, \exp(-\Delta E_i^{(k)}/T_k)\}$. Annealing schedules used to lower the temperature often have T_k that is proportional to $1/k$ or $1/\log k$. See Bertsimas and Tsitsiklis (1993); Geman and Geman (1984); Hajek (1988), and Wang et al. (2016).

3.2 Quantum annealing

As in the classical annealing method, graph $\mathcal{G}$ is used to describe the quantum Ising model while the vertex set $\mathcal{V}(\mathcal{G})$ represents the quantum spins, and the edge set $\mathcal{E}(\mathcal{G})$ denotes the couplings (or interactions) between two quantum spins. Since qubits can be used to realize quantum spins, each vertex can be represented by a qubit. Given b vertices in $\mathcal{G}$, the quantum system is characterized by a d-dimensional complex space where $d = 2^b$. The quantum state is described by a unit vector in $\mathbb{C}^d$, and its dynamic evolution is governed by the Schrödinger equation defined in (2.1) via a quantum Hamiltonian. The Hamiltonian here is a Hermitian matrix of size d. The eigenvalues of the quantum Hamiltonian are connected with the energies of the quantum system, and the eigenvector corresponds to the smallest eigenvalue represents a ground state.

$$\mathbf{I}_j = \begin{pmatrix} 1 & 0 \\ 0 & 1 \end{pmatrix}, \quad \boldsymbol{\sigma}_j^x = \begin{pmatrix} 0 & 1 \\ 1 & 0 \end{pmatrix}, \quad \boldsymbol{\sigma}_j^z = \begin{pmatrix} 1 & 0 \\ 0 & -1 \end{pmatrix}, \qquad j = 1, \ldots, b,$$

where $\boldsymbol{\sigma}_j^x$ and $\boldsymbol{\sigma}_j^z$ are Pauli matrices in x and z axes, respectively. We note that the Pauli matrix in y axis is not needed (Nielsen and Chuang, 2000; Wang, 2012). For the quantum system, each classical vertex variable $s_j = \pm 1$ in (3.2) is replaced by $\boldsymbol{\sigma}_j^z$ for the jth quantum spin, which is further realized by a qubit. The two eigenvalues ± 1 of the Pauli matrix $\boldsymbol{\sigma}_j^z$ correspond to the eigenstates $|+1\rangle$ and $|-1\rangle$ where each further represents the spin up state $|\uparrow\rangle$ and spin down state $|\downarrow\rangle$. In total, there are 2^b possible quantum configurations made by combining the $2b$ eigenstates in the form $|\pm 1\rangle$ of the Pauli matrices $\{\boldsymbol{\sigma}_j^z\}_{j=1}^b$. We replace s_j in the classical Ising Hamiltonian $\mathbf{H}_I^c(\mathbf{s})$ by $\boldsymbol{\sigma}_j^z$ to obtain the quantum version, that is,

$$\mathbf{H}_I^q = -\sum_{(i,j)\in\mathcal{E}(\mathcal{G})} J_{ij}\boldsymbol{\sigma}_i^z\boldsymbol{\sigma}_j^z - \sum_{j\in\mathcal{V}(\mathcal{G})} h_j\boldsymbol{\sigma}_j^z, \tag{3.4}$$

where J_{ij} is the Ising coupling along the edge $(i,j) \in \mathcal{E}(\mathcal{G})$, and h_j is the local field on the vertex $j \in \mathcal{V}(\mathcal{G})$. Here we follow the convention in quantum literature so that $\boldsymbol{\sigma}_j^z$ and $\boldsymbol{\sigma}_i^z\boldsymbol{\sigma}_j^z$ in (3.4) stand for their tensor products along with identical matrices

$$\boldsymbol{\sigma}_i^z\boldsymbol{\sigma}_j^z \equiv \mathbf{I}_1 \otimes \cdots \otimes \mathbf{I}_{i-1} \otimes \underbrace{\boldsymbol{\sigma}_i^z \otimes \mathbf{I}_{i+1} \otimes \cdots \otimes \mathbf{I}_{j-1} \otimes \boldsymbol{\sigma}_j^z}_{\text{vertices } i \text{ and } j} \otimes \mathbf{I}_{j+1} \otimes \cdots \otimes \mathbf{I}_b,$$

$$\boldsymbol{\sigma}_j^z \equiv \mathbf{I}_1 \otimes \cdots \otimes \underbrace{\mathbf{I}_{j-1} \otimes \boldsymbol{\sigma}_j^z \otimes \mathbf{I}_{j+1}}_{\text{vertex } j} \otimes \cdots \otimes \mathbf{I}_b.$$

Each term in (3.4) is a tensor product of b matrices of size two and as a result, all terms in $\mathbf{H}_I^q$ are diagonal matrices of size 2^b, and so does $\mathbf{H}_I^q$. We have one matrix to act on the jth qubit, either a Pauli matrix $\boldsymbol{\sigma}_j^z$ or an identity matrix $\mathbf{I}_j$. The quantum convention identifies the qubits with Pauli matrices for real actions but omits the identical matrices and tensor product signs.

To find a quantum spin configuration with the minimal energy, or equivalently, a ground state of quantum Hamiltonian $\mathbf{H}_I^q$, we need to search for an eigenvector of $\mathbf{H}_I^q$ corresponding to its smallest eigenvalue. We note that $\mathbf{H}_I^q$ involves only commuting diagonal matrices, and its eigenvalues are equal to its diagonal entries, which in turn are the 2^b possible values of classical Hamiltonian $\mathbf{H}_I^c(\mathbf{s})$. Thus, the quantum system governed by $\mathbf{H}_I^q$ behaves essentially like a classical system and finding the minimal energy of the quantum Ising Hamiltonian $\mathbf{H}_I^q$ is equivalent to finding the minimal energy of the classical Ising Hamiltonian $\mathbf{H}_I^c$. This result is established mathematically in the following theorem.

Theorem 1 *Suppose that the classical and quantum Ising models have respective Hamiltonians $\mathbf{H}_I^c$ and $\mathbf{H}_I^q$ described by the same graph $\mathcal{G}$ with b vertices, the identical couplings J_{ij} and local fields h_j. Then the quantum Ising model governed by $\mathbf{H}_I^q$ has the same Boltzmann distribution of observing configurations as the classical Ising model governed by $\mathbf{H}_I^c$, and finding the minimal energy of the quantum Ising model is mathematically identical to finding the minimal energy of the classical Ising model.*

Remark 2 *Theorem 1 indicates that the original optimization problem described in Section 3.1 can be formulated in the quantum framework, and the computational task for solving the optimization problem remains the same as in the classical case.*

To carry out quantum annealing, it is essential to engineer a transverse magnetic field that is orthogonal to the Ising axis and obtain the corresponding Hamiltonian in the transverse field. The transverse field represents kinetic energy that doe not commute with the potential energy $\mathbf{H}_I^q$, therefore, it induces transitions between the up and down states of every single spin, and converts the system behavior from classical to quantum. Assume that the following quantum Hamiltonian governs the transverse magnetic field

$$\mathbf{H}_X = -\sum_{j\in\mathcal{V}(\mathcal{G})} \boldsymbol{\sigma}_j^x, \tag{3.5}$$

where $\boldsymbol{\sigma}_j^x$ denotes the tensor products of b matrices of size 2,

$$\boldsymbol{\sigma}_j^x \equiv \mathbf{I}_1 \otimes \cdots \otimes \underbrace{\mathbf{I}_{j-1} \otimes \boldsymbol{\sigma}_j^x \otimes \mathbf{I}_{j+1}}_{\text{vertex } j} \otimes \cdots \otimes \mathbf{I}_b, \tag{3.6}$$

and does not commute with $\boldsymbol{\sigma}_j^z$ in $\mathbf{H}_I^q$. We note that $\boldsymbol{\sigma}_j^x$ has two eigenvalues $+1$ and -1 and each one is associated with the eigenvector $|\mathbf{v}_{j,1}\rangle = (1,1)^\dagger$ and $|\mathbf{v}_{j,-1}\rangle = (1,-1)^\dagger$. As a result, the eigenvector corresponds to the smallest eigenvalue of $\mathbf{H}_X$ is $|\mathbf{v}_+\rangle = |\mathbf{v}_{1,+1}\rangle \otimes |\mathbf{v}_{2,+1}\rangle \otimes \cdots \otimes |\mathbf{v}_{b,+1}\rangle$, and $|\mathbf{v}_+\rangle$ is the ground state of $\mathbf{H}_X$.

We start the quantum annealing procedure with a quantum system that is driven by the transverse magnetic field $\mathbf{H}_X$ and is initialized in its ground state $|\mathbf{v}_+\rangle$. The system then gradually evolves from the initial Hamiltonian $\mathbf{H}_X$ to its final target Hamiltonian $\mathbf{H}_I^q$. During the Hamiltonian change, the system tends to stay in the ground states of the instantaneous Hamiltonian via quantum tunneling based on the adiabatic quantum theorem (Farhi et al., 2000, 2001, 2002; McGeoch, 2014). At the end of the annealing procedure, if the quantum system stays in a ground state of the final Hamiltonian $\mathbf{H}_I^q$, we are able to obtain an optimal solution by measuring the system.

In specific, quantum annealing is realized by an instantaneous Hamiltonian for the Ising model in the transverse field as follows,

$$\mathbf{H}_D(t) = A(t)\mathbf{H}_X + B(t)\mathbf{H}_I^q, \qquad t \in [0, t_f], \tag{3.7}$$

where $A(t)$ and $B(t)$ are smooth functions depend on time t that control the annealing schedules, and t_f is the total annealing time. To drive the system from $\mathbf{H}_X$ to $\mathbf{H}_I^q$, we take $A(t_f) = B(0) = 0$ where $A(t)$ is decreasing and $B(t)$ is increasing. It follows that when $t = 0$, $\mathbf{H}_D(0) = A(0)\mathbf{H}_X$ and when $t = t_f$, $\mathbf{H}_D(t_f) = B(t_f)\mathbf{H}_I^q$. Since $A(0)$ and $B(t_f)$ are known scalars, $\mathbf{H}_D(t)$ has the same eigenvectors as $\mathbf{H}_X$ at the initial time $t = 0$ and as $\mathbf{H}_I^q$ at the final time $t = t_f$, where the corresponding eigenvalues differ by factors of $A(0)$ and $B(t_f)$, respectively. Therefore, $\mathbf{H}_D(t)$ moves the system from $\mathbf{H}_X$ initialized in its ground state to the final target $\mathbf{H}_I^q$. When the control functions $A(t)$ and $B(t)$ are chosen appropriately, the quantum adiabatic theorem indicates that the annealing procedure driven by (3.7) will have a sufficiently high probability in finding the global minimum of $\mathbf{H}_I^c(\mathbf{s})$ and solving the minimization problem at the final annealing time t_f. The following theorem provides the probability lower bound on successfully solving the optimization problem at the final annealing time t_f by quantum annealing.

Theorem 3 *Suppose that the quantum system associated with quantum annealing is driven by* $\mathbf{H}_{QA}(t) = A(t)\mathbf{H}_0 + B(t)\mathbf{H}_1$, $t \in [0, t_f]$, *where* $t_f > 0$, $\mathbf{H}_0$ *and* $\mathbf{H}_1$ *are two quantum Hamiltonians, annealing schedules* $A(t)$ *and* $B(t)$ *are smooth functions and satisfy* $A(t_f) = B(0) = 0$, $A(t)$ *is decreasing and* $B(t)$ *is increasing, and the system is initialized in a ground state of* $\mathbf{H}_0$ *at* $t = 0$. *The probability that the lowest energy of* $\mathbf{H}_1$ *is obtained by measuring the system at the end of the annealing procedure is then bounded from below by*

$$e^{-\xi} - 2^b \zeta \Pi e^{2\xi}(1 - p_0), \tag{3.8}$$

where ζ *is the number of ground states,* p_0 *is a constant such that* $p_0 \in [0, 1]$,

$$\Pi = \max\left\{ \left| \frac{1}{\lambda_j(u) - \lambda_0(u)} \langle 0^{(\ell)}(u)| \frac{d\mathbf{H}_{QA}(ut_f)}{du} |j(u)\rangle \right|^2, j \geq 1, \ell = 1, \ldots, \zeta, u \in [0, 1] \right\},$$

$\lambda_j(u)$, $j = 0, 1, 2, \ldots$, *are eigenvalues of* $\mathbf{H}_{QA}(ut_f)$ *listed in an increasing order, and* $|0^{(\ell)}(u)\rangle$, $\ell = 1, \ldots, \zeta$ *are the ground states corresponding to the smallest eigenvalue* $\lambda_0(u)$, *with* $|j(u)\rangle$ *any normalized eigenvector corresponding to eigenvalue* $\lambda_j(u)$, $j \geq 1$, $u \in [0, 1]$, $A(u) = (A_{\ell l}(u))$ *is a* ζ *by* ζ *matrix given by* $A_{\ell l}(u) = -\sqrt{-1}\langle \check{0}^{(\ell)}(u)| \frac{d}{du} \check{0}^{(l)}(u)\rangle$ *for* $\ell \neq l$ *and* 0 *for* $\ell = l$,

$$\xi = \int_0^1 \|A(u)\| du \left(1 - \frac{1}{\pi} \int_0^1 \|A(u)\| du\right)^{-1},$$

and $\|A(u)\|$ *is the spectral norm of* $A(u)$. *In particular, if there is a unique ground state, then* $\zeta = 1$ *and* $\xi = 0$, *the probability lower bound in* (3.8) *becomes to* $1 - 2^b \Pi(1 - p_0)$.

The ground state success probability of quantum annealing is usually derived under the unique ground state condition in an asymptotic sense, that is, we obtain some expressions or bounds for the leading terms of the ground state success probability by taking t_f to go to infinity (Aharonov et al., 2008; Born and Fock, 1928; McGeoch, 2014; Morita and Nishimori, 2008). We provide the probability lower bound in (3.8) that is for finite t_f and does not impose the unique ground state restriction. From the proof, p_0 can be interpreted as the probability that the quantum system stays in a ground state during the annealing procedure. We note that

$$\frac{d\mathbf{H}_{QA}(u\, t_f)}{du} = \frac{dA(u\, t_f)}{du}\, \mathbf{H}_0 + \frac{dB(u\, t_f)}{du}\, \mathbf{H}_1,$$

depends on u only through the derivatives of annealing schedules $A(t)$ and $B(t)$. By choosing $A(t)$ and $B(t)$ appropriately, we can make the probability lower bound in (3.8) away from zero and thus, guarantee that quantum annealing can find the lowest energy of $\mathbf{H}_1$ with some probability. In Theorem 3, we may take $\mathbf{H}_0 = \mathbf{H}_X$ given by (3.5), $\mathbf{H}_1 = \mathbf{H}_I^q$ defined in (3.4), and $\mathbf{H}_{QA} = \mathbf{H}_D$ in (3.7), then by Theorems 1 and 3 together, we conclude that the quantum annealing driven by (3.7) can find the global minimum of $\mathbf{H}_I^c(\mathbf{s})$ and solve the minimization problem with certain probability.

3.3 Simulated Quantum Annealing with path-integral Monte Carlo method

In this section, we discuss how to employ classical Monte Carlo method to mimic the behavior of quantum annealing and derive relevant theoretical results. Metropolis-Hastings algorithm is one of the most popular ways to generate the Markov chain and we review the homogeneous case first. To obtain random samples from the target probability distribution $q(x)$ using the Metropolis-Hastings, we first choose an arbitrary point $x^{(0)}$ and then generate a candidate $y^{(0)}$ for the next sample using the generation probability $P(y, x^{(0)})$ which is symmetric, that is, $P(x, y) = P(y, x)$. We accept $y^{(0)}$ as the next sample $x^{(1)}$ with acceptance probability $A(y^{(0)}, x^{(0)})$ and reject $y^{(0)}$ with probability $1 - A(y^{(0)}, x^{(0)})$. One common choice of the acceptance probability is $A(y, x) = \min(1, q(y)/q(x))$. We repeat the above algorithms and obtain the sequence of random samples from $q(x)$. Specifically, Algorithm 1 summarizes the Metropolis-Hastings algorithm.

Algorithm 1 Metropolis-Hastings Algorithm

Input:

(1) Initial state $x^{(0)}$;

(2) Generation probability $P(y, x)$;

(3) Acceptance probability $A(y, x)$.

1: Generate $y_t \sim P(y, x^{(t)})$;

2: Take

$$x^{(t+1)} = \begin{cases} y^{(t)} & \text{with probability } A(y^{(t)}, x^{(t)}) \\ x^{(t)} & \text{with probability } 1 - A(y^{(t)}, x^{(t)}). \end{cases}$$

The transition probability of the Metropolis-Hastings is given by

$$G(y, x) = P(y, x)A(y, x)$$

while the sufficient condition of existing stationary distribution $q(x)$ is detailed balance, that is,

$$G(y, x)q(x) = G(y, x)q(y).$$

We extend above homogeneous Markov chain to the inhomogeneous Markov chain and apply the path-integral method to the d-dimensional transverse magnetic field Ising model. We define the transition probability that characterizes a Monte Carlo. For an Ising model that has b sites, we let

$$\begin{aligned} q_{M,\beta}(\mathbf{s}, t) &= \frac{1}{Z_{M,\beta}(t)} \exp\left(\beta F_{0,M}(\mathbf{s}) + \gamma_\beta(t) F_{1,M}(\mathbf{s})\right), \\ Z_{M,\beta}(t) &= \sum_{\mathbf{s} \in \{-1,1\}^{bM}} \exp\left(\beta F_{0,M}(\mathbf{s}) + \gamma_\beta(t) F_{1,M}(\mathbf{s})\right); \end{aligned}$$

$$q_{M,\beta}(\mathbf{s}) = \frac{1}{Z_{M,\beta}} \exp\left(\beta F_{0,M}(\mathbf{s})\right), \qquad Z_{M,\beta} = \sum_{\mathbf{s}\in\{-1,1\}^{bM}} \exp\left(\beta F_{0,M}(\mathbf{s})\right),$$

where

$$F_{0,M}(\mathbf{s}) = \frac{1}{M}\sum_{k=1}^{M}\sum_{\langle ij\rangle} J_{ij}s_{i,k}s_{j,k}, \qquad F_{1,M}(\mathbf{s}) = \sum_{k=1}^{M}\sum_{i=1}^{b} s_{i,k}s_{i,k+1},$$
$$\gamma_\beta(t) = \frac{1}{2}\log\left(\coth\frac{\beta\Gamma(t)}{M}\right).$$

We define the transition probability from state $x \in \{-1,1\}^{bM}$ to state $y \in \{-1,1\}^{bM}$ at time step t as follows

$$G(y,x;t) = \begin{cases} P(y,x)A(y,x;t) & \text{if } x \neq y \\ 1 - \sum_{z\notin x} P(z,x)A(z,x;t) & \text{if } x = y \end{cases} \tag{3.9}$$

where $P(y,x)$ is the generation probability and $A(y,x;t)$ is the acceptance probability. Specifically, $P(y,x)$, the probability to generate the next candidate state y from the present state x, satisfies the following conditions

(1) $\forall x, y \in \{-1,1\}^{bM} : P(y,x) = P(x,y) \geq 0$;

(2) $\forall x \in \{-1,1\}^{bM} : \sum_{y\in\{-1,1\}^{bM}} P(y,x) = 1$;

(3) $\forall x \in \{-1,1\}^{bM} : P(x,x) = 0$;

(4) $\forall x, y \in \{-1,1\}^{bM}, \exists n > 0, \exists z_1, \ldots, z_{n-1} \in \{-1,1\}^{bM} : \prod_{k=0}^{n-1} P(z_{k+1}, z_k) > 0, z_0 = x, z_n = y$.

$A(y,x;t)$, the acceptance probability, is defined as

$$A(y,x;t) = g\left(\frac{q_{M,\beta}(y,t)}{q_{M,\beta}(x,t)}\right).$$

where the acceptance function $g(u)$ satisfies (i) monotone increasing, (ii) $0 \leq g(u) \leq 1$, and (iii) $g(1/u) = g(u)/u$. Examples include $u/(1+u)$ and $\min(1,u)$. Given above set-up, $q_{M,\beta}(y,t)$ satisfies the detailed balance condition, that is,

$$G(y,x;t)q_{M,\beta}(x,t) = G(x,y;t)q_{M,\beta}(y,t).$$

For a fixed t, $q_{M,\beta}(x,t)$ is then the stationary distribution of the homogeneous Markov chain defined by the transition matrix $(G(x,y;t))_{x,y}$.

To establish the theoretical results, we define

$$R = \min\{\max\{d(y,x) : y \in \{-1,1\}^{bM}\} : x \in \{-1,1\}^{bM} \setminus S_m\},$$
$$L_{1,M} = \max\left\{|F_{1,M}(x) - F_{1,M}(y)| \ : \ P(y,x) > 0,\ x, y \in \{-1,1\}^{bM}\right\},$$

where

$$S_m = \{x : x \in \{-1,1\}^{bM}, F_{1,M}(y) \le F_{1,M}(x), \forall y \in \{-1,1\}^{bM} \text{ and } P(y,x) > 0\},$$

and $d(y,x)$ denotes the minimum number of steps necessary to make a transition from x to y, $P(y,x)$ is defined in (3.9). We first consider the marginal distribution. Let

$$q^1_{M,\beta}(\mathbf{s_1}, t) = \sum_{k=2}^{M} \sum_{\mathbf{s_k}} q_{M,\beta}(\mathbf{s}, t), \qquad q^1_{M,\beta}(\mathbf{s}_1) = \sum_{k=2}^{M} \sum_{\mathbf{s_k}} q_{M,\beta}(\mathbf{s}),$$

where $\mathbf{s_k} = \{s_{i,k}, i = 1, \ldots, b\}$ and $\mathbf{s} = \cup_{k=1}^{M} \mathbf{s}_k$.

Lemma 4 *Suppose*

$$\Gamma(t) \ge \frac{M}{\beta} \tanh^{-1} \frac{1}{(t+2)^{2/(RL_{1,M})}}.$$

Then $q^1_{M,\beta}(\mathbf{s_1}, t)$ with β and $q_{1,\beta/M}(\mathbf{s_1}, t)$ with β/M are asymptotically the same as $t \to \infty$.

Let

$$X_M(t) = \frac{1}{\sqrt{M}} \sum_{k=1}^{M} \sum_{\langle ij \rangle} J_{ij} s_{i,k} s_{j,k},$$

where $\mathbf{s}$ is generated by $q_{M,\beta}(\mathbf{s}, t)$.

Theorem 5 *For any given $\epsilon > 0$, there are X_∞ and $M_0(\epsilon)$ such that for any given $M \ge M_0(\epsilon)$, there is $t_0(\epsilon, M)$ such that for all $t \ge t_0(\epsilon, M)$ and any $x \in \mathbb{R}$,*

$$|P(X_M(t) \le x) - P(X_\infty \le x)| < \epsilon,$$

if

$$\Gamma(t) \ge \frac{M}{\beta} \tanh^{-1} \frac{1}{(t+2)^{2/(RL_{1,M})}},$$

where $X_\infty \sim N(0, \sum_{\langle ij \rangle} J_{ij}^2)$.

Remark 6 *The marginal distribution of $\mathbf{s}_k$ has the probability mass function (PMF)*

$$P(\mathbf{s}_k = s_k) = \frac{1}{Z_{\beta/M}} \exp\left(\frac{\beta}{M} \sum_{\langle ij \rangle} J_{ij} s_{i,k} s_{j,k} \right).$$

By Taylor expansion, we have

$$Z_{\beta/M} = \sum_{\mathbf{s}} \left(1 + \frac{\beta}{M} \sum_{\langle ij \rangle} J_{ij} s_i s_j + O(M^{-2}) \right) = 2^b + O(M^{-2})$$

and

$$\exp\left(\frac{\beta}{M}\sum_{\langle ij\rangle} J_{ij}s_{i,k}s_{j,k}\right) = 1 + \frac{\beta}{M}\sum_{\langle ij\rangle} J_{ij}s_{i,k}s_{j,k} + O(M^{-2}),$$

which implies that $P(\mathbf{s}_k = s_k)$ *converges to the discrete uniform distribution as* $M \to \infty$. *That is,*

$$P(\mathbf{s}_k = s_k) \to \frac{1}{2^b} \quad \text{as } M \to \infty.$$

Then $\mathbf{s}_k$ *has mean zero and variance* $\sum_{\langle ij\rangle} J_{ij}^2$ *as* $M \to \infty$.

Note: please check, $\mathbf{s}_k \sim q_{M,\beta}(s)$

Lemma 7 *For given* t, *we have*

$$\left|\left(\sqrt{\frac{1}{2}\sinh\frac{2\beta\Gamma(t)}{M}}\right)^{bM} Z_{M,\beta}(t) - Z_\beta(t)\right| = O((\beta/M)^2),$$

where $Z_\beta(t) = Tr\left(\exp\left(\beta\sum_{\langle ij\rangle} J_{ij}\sigma_i^z\sigma_j^z + \beta\Gamma(t)\sum_i \sigma_i^x\right)\right)$.

4 Numerical analysis

4.1 Quantum annealing by D-Wave machine

We investigate data collected from annealing experiments conducted by D-Wave (DW) machine where the number of qubits used equals to either 485 or 1094. That is, we consider an Ising model with b spins where $b = 485$ or 1094. The Ising model studied in this paper took external magnetic field $h_j = 0$ so that the optimization problem could be easier. Within each experiment, to create a problem instance, we randomly assigned a value of either $+1$ or -1 to each coupler J_{ij} in the DW machine. The same procedure was repeated for 100 times so that in total, 100 problem instances each with a random assignment of couplings $\{J_{ij}, (i,j) \in \mathcal{E}(\mathcal{G})\}$ where $J_{ij} = \pm 1$, were obtained. For each of the 100 selected instances, after its couplings were programmed, 1000000 annealing runs were performed on the DW machine. The energy level at the end of each annealing run was recorded. Theorem 1 and 3 guarantee that the quantum annealing can find the global minimum of $\mathbf{H}_I^c(\mathbf{s})$ by measuring the quantum system at the end of each annealing run with a positive probability. To determine whether the system has found the global minimum or reached the ground state, we adopt the following annealing method: given a problem instance, we declare that a particular annealing run obtains the ground state if the final energy level recorded is the same as the global minimum energy level for the problem instance, $\mathbf{H}_I^c(\mathbf{s})$. For each of the 100 selected instances, we were able to determine whether the ground state has been achieved during a particular run out of 1000000 runs. We recorded the frequency of finding the ground state among 1000000 runs and computed its corresponding probability, that is, the

ground state success probability. Figure 1 presents the histogram plot that consists of the 100 ground state success probabilities for the 100 problem instances under the circumstances where $b = 485$ and $b = 1094$. Both histograms exhibit unimodal shape. For $b = 485$, ground state success probability ranges from 0.00024 to 0.28502 while for $b = 1094$, ground state success probability ranges from 0.0001 to 0.00371. As the number of qubits increases, the DW machine finds it harder to reach minimum energy level given various problem instances as the interactions among couplers become more complicated.

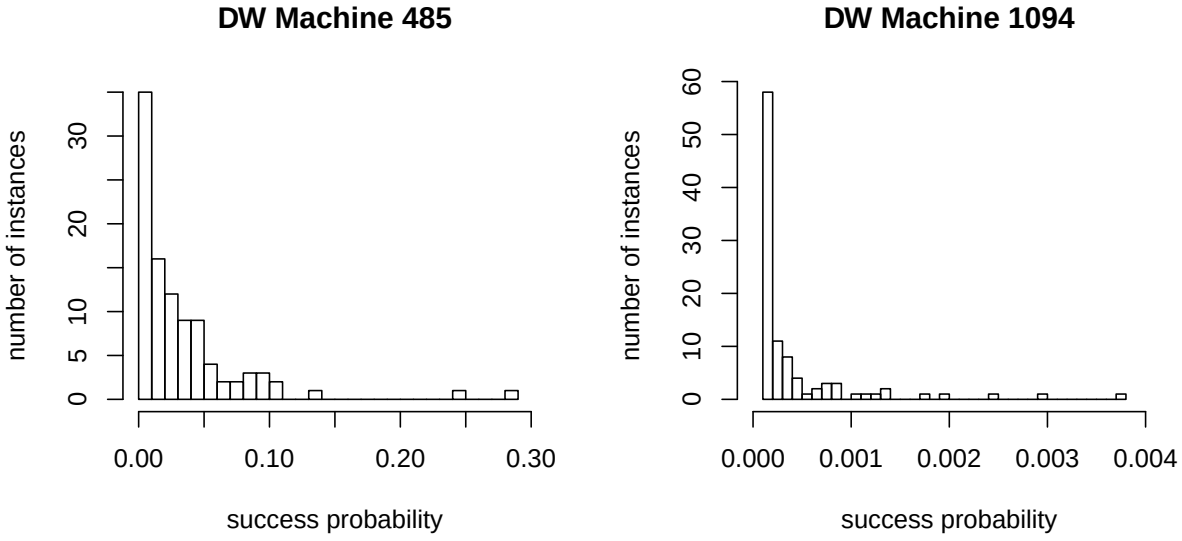

Figure 1: Histogram plot of ground state success probability data collected from DW machine consist of 100 problem instances.

4.2 SA and SQA via MCMC method

We approximate quantum annealing with classical path-integral Monte Carlo method described in Section 3.3. The SQA procedure assumes a Chimera graph where the total number of qubits is b. For the quantum annealing Hamiltonian $\mathbf{H}_D(t)$ in (3.7), to find the Boltzmann state of the quantum system, we are required to evaluate canonical partition function $\mathrm{tr}[e^{-\mathbf{H}_D(t)/T}]$ for the transverse field quantum Ising model. To approximate the partition function, we use the Trotter formula (Kato, 1978; Suzuki, 1976; Trotter, 1959). Specifically, given annealing schedules $A(t)$ and $B(t)$ from quantum annealing and to approximate the partition function for quantum annealing Hamiltonian $\mathbf{H}_D(t)$ with temperature T, we replace the temperature parameter by $T/B(t)$ and the transverse field parameter by $A(t)/B(t)$. Such approximation maps the transverse quantum Ising model to a classical $(2 + 1)$-dimensional

anisotropic Ising model with temperature τT and Hamiltonian

$$\mathbf{H}_{aI}^{c}(\mathbf{s}) = -\sum_{l=1}^{\tau}\left[B(t)\sum_{(i,j)\in\mathcal{E}(\mathcal{G})}J_{ij}s_{il}s_{jl} + J(t)\sum_{j\in\mathcal{V}(\mathcal{G})}s_{jl}s_{j,l+1}\right]$$

where $s_{il} = \pm 1$ are random variables, τ is an integer, J_{ij} are the regular couplings along the original 2-dimensional direction of the Ising model and l is the index for an extra dimension that is often referred to as the imaginary-time dimension with

$$J(t) = -\frac{\tau T}{2}\ln\left[\tanh\left(\frac{A(t)}{\tau T}\right)\right]$$

as the coupling along the imaginary-time direction.

Let $\mathbf{s}_l = \{s_{il}, l = 1,\ldots,b\}$, $1 \le l \le \tau$ be the lth Trotter slice correponding to one particular configuration. We now transform the original 2-dimensional transverse quantum Ising model to a classical (2+1)-dimensional Ising model with the additional dimension in imaginary-time. The imaginary-time dimension has a finite length τ, uniform coupling and an annealing schedule $J(t)$. Given the classical anisotropic Ising Hamiltonian $\mathbf{H}_{aI}^{c}$, we are allowed to approximate the transverse field quantum Ising model by a classical path-integral Monte Carlo method. With the additional dimension in imaginary-time, the Monte Carlo simulation needs to adopt a standard Metropolis-Hastings algorithm both in local and global moves. For the local moves, we perform usual independent spin flips for all spins embedded within all Trotter slices while for the global moves, we attemp to flip all the replicas of the same spin embedded within all Trotter slices.

We start the SQA algorithm by randomly assigning ± 1 values independently to all spins embeded within all Trotter slices. The initial spin configuraion is denoted as $\mathbf{s}^{(0)} = \{s_{jl}^{(0)}, j \in \mathcal{V}(\mathcal{G}), l = 1,\ldots,\tau\}$. We update spins one by one for local moves and spin replicas site by site for global moves. We call a complete update of all spins both in local and global moves a sweep and denote the total number of sweeps as R. Let $t_k = k/R$, $k = 1,\ldots,R$. For the kth local sweep, we focus on spin i in the lth Trotter slice while keeping all the other spins the same. The energy change from state $s_{il}^{(k-1)}$ to a new state $s_{il}^{(k)} = -s_{il}^{(k-1)}$ is

$$\begin{aligned}\triangle E_{1il}^{(k)} &= -B(t_k)\left[\sum_{j=1}^{i-1}J_{ij}s_{jl}^{(k)}\left(s_{il}^{(k)} - s_{il}^{(k-1)}\right) + \sum_{j=i+1}^{b}J_{ij}s_{jl}^{(k-1)}\left(s_{il}^{(k)} - s_{il}^{(k-1)}\right)\right] \\ &\quad -J(t_k)\left[s_{il}^{(k)}s_{i,l+1}^{(k)} + s_{i,l-1}^{(k)}s_{il}^{(k)} - s_{il}^{(k-1)}s_{i,l+1}^{(k-1)} - s_{i,l-1}^{(k-1)}s_{il}^{(k-1)}\right]\end{aligned}$$

and the new state $s_{il}^{(k)}$ is accepted with probability $\min\left\{1, \exp\left[-\triangle E_{1il}^{(k)}/(\tau T)\right]\right\}$ during the kth local sweep. On the other hand, for the kth global sweep, we attempt to flip spins at site i embedded within all Trotter slices l, $l = 1,\ldots,\tau$. The energy change from state $\{s_{il}^{(k-1)}, l = 1,\ldots,\tau\}$ to state $\{s_{il}^{(k)} = -s_{il}^{(k-1)}, l = 1,\ldots,\tau\}$ is

$$\triangle E_{2i}^{(k)} = -\sum_{l=1}^{\tau}B(t_k)\left[\sum_{j=1}^{i-1}J_{ij}s_{jl}^{(k)}\left(s_{il}^{(k)} - s_{il}^{(k-1)}\right) + \sum_{j=i+1}^{b}J_{ij}s_{jl}^{(k-1)}\left(s_{il}^{(k)} - s_{il}^{(k-1)}\right)\right]$$

and the new state $s_{il}^{(k)}$ is accepted with probability $\min\left\{1, \exp\left[-\triangle E_{2i}^{(k)}/(\tau T)\right]\right\}$ during the kth global sweep. To evaluate the original classical Hamiltonian $\mathbf{H}_I^c(\mathbf{s})$ in (3.2), we simply plug in the configuration $\mathbf{s}^{(k)} = \{s_i^{(k)}, i \in \mathcal{V}(\mathcal{G})\}$ obtained from the first Trotter slice at the last sweep and take $h_j = 0$. The SQA method based on path-integral Monte Carlo simulation studies the 2-dimensional transverse field quantum Ising model through a (2+1)-dimensional classical Ising model and brought the system to an equilibrium state at each sweep under the Metropolis-Hastings algorithm.

We now take a Chimera graph that is close to the one adopted by DW machine where the total number of spins b equals to either 485 or 945 that is comparable to the total number of qubits studied in previous Section 4.1. We create 100 problem instances by randomly assigning ± 1 to all spins and take the following annealing schedules closed to the DW annealing schedules

$$A(t) = \begin{cases} 8t^2 - 9.6t + 2.88, & \text{if } 0 \leq t \leq 0.6 \\ 0, & \text{if } 0.6 < t <\leq 1 \end{cases}$$

$$B(t) = 5.2t^2 + 0.2t, \quad t \in [0, 1].$$

We take temperature T to be 0.1 and number of Trotter slices τ to be either 30 or 60. Let the total number of sweeps for SQA method to be 100000, 200000 and 500000. For each of the 100 problem instances, we ran the SQA algorithm for 3000 times and for each annealing run, we declare that the particular run finds its ground state if the run yields a minimum value that is the same as the known global minimum of $\mathbf{H}_I^c(\mathbf{s})$ for the instance. The global minimum values are determined by SA algorithms described in Section 3.1 where for each assigned problem instance, we run the algorithm with the following number of sweeps: 1000000, 5000000 and 10000000, each for 3000 times. For a specific problem instance, out of the 9000 SA runs, the minimum energy level reported is considered to be the global minimum energy level.

Figure 2 and 3 present the histograms for ground state success probability data obtained by the SA method and SQA method, respectively. Given the same 100 problem instances and global minimum energy levels reported by SA, the SA on average has a higher probability of finding the minimum values comparing to SQA. For the SA method, the histograms exhibit uniform pattern when $b = 485$ and unimodal pattern when $b = 945$ for all sweep numbers. As the number of sweeps increases, the ground state success probability increases on average so that the patterns become weaker. For the SQA method, the histograms exhibit similar unimodal patterns for all sweep and slice numbers. The additional number of slices made it more difficult for the SQA to find the minimum energy level given our current sweep numbers comparing to the SA. For each slice number, ground state success probability increases as the sweep number increase for most of the 100 problem instances so that in general, the unimodal pattern becomes weaker as the sweep number increases. For each sweep number, ground state success probability decreases as the slices number changes from 30 to 60 for most of the 100 problem instances so that in general, the unimodal pattern becomes stronger as the slices number changes from 30 to 60. The histograms for ground state success probability

obtained by the SQA method share the similar pattern with the histogram generated by the DW machine. However, the success probability obtained by SQA method ranges from 0 to 0.8 when the number of spins equals to 485 and ranges from 0 to 0.45 when the number of spins equals to 945 while the success probability generated by DW machine ranges from 0 to 0.3.

(a) total number of spins: 485

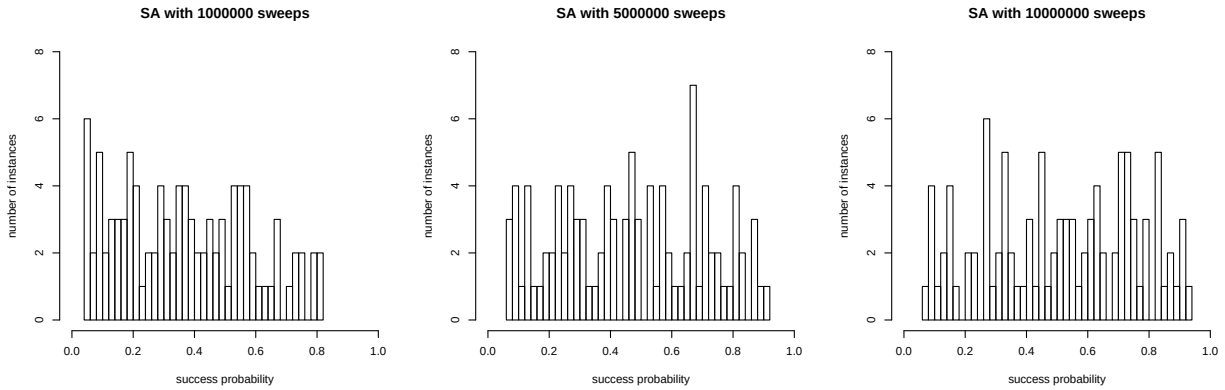

(b) total number of spins: 945

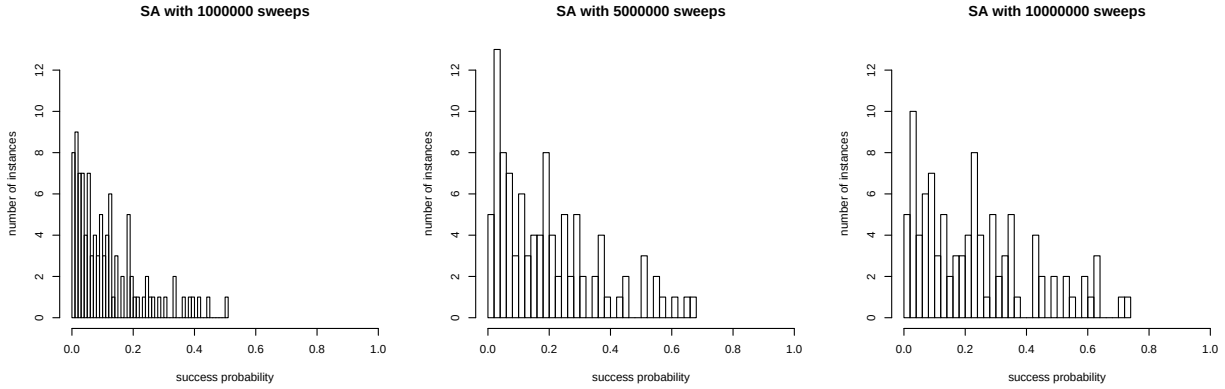

Figure 2: Histogram plots of ground state success probability data based on SA algorithm for 100 problem instances.

5 Concluding remarks

Quantum computation has drawn enormous attention in many frontiers of multiple scientific fields and can give rise to an exponential speedup over classical computers in solving certain computational problems. Since statistics and machine learning nowadays involve computation work heavily, there is a great demand in studying statistical issues for theoretical research and experimental work with quantum computers.

(a) total number of spins: 485

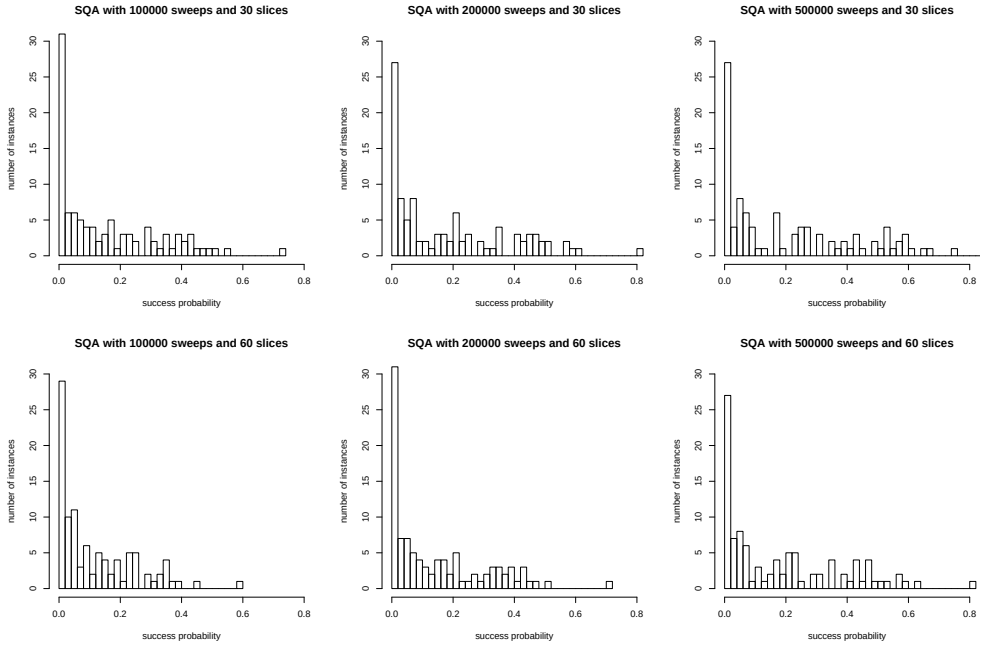

(b) total number of spins: 945

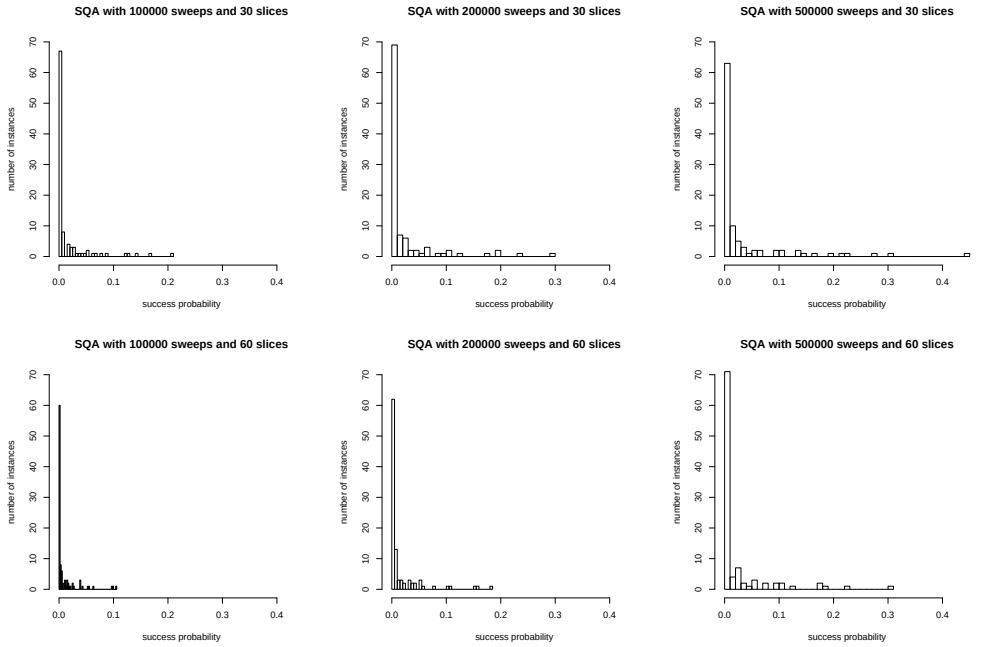

Figure 3: Histogram plots of ground state success probability data based on SQA algorithm for 100 problem instances.

This paper reviews classical annealing such as simulated annealing, discusses quantum annealing that is implemented by D-Wave computing devices and by MCMC based annealing methods. We show that if the classical and quantum annealing are characterized by equivalent Ising models, then solving an optimization problem by the two annealing procedures are mathematically identical. Moreover, we derive the probability lower bound of finding the minimal energy, or equivalently, solving the optimization problem, through quantum annealing by measuring the system at the end of the annealing procedure. Attempts to quantify the quantum nature of the D-Wave devices have been not only met with excitement but also confronted with suspicion. Wang et al. (2016) studied the consistency or inconsistency between data obtained from D-Wave devices and gathered through MCMC based annealing methods where the total number of qubits is 100, which is relatively small. In this paper, we demonstrate that fundamental distinguishment exists between the classical and quantum annealing methods when the total number of qubits involved is at the level of 500 or 1000. The results provide strong evidence that the input-output data of D-Wave devices are inconsistent with the statistical behaviors of the MCMC-based annealing models.

6 Appendix: Proofs

Denote C's the generic constants whose values are free of m, n, M, d and may change from appearance to appearance.

6.1 Proof of Theorem 1

Let $\mathbf{e}_{j,+1} = (1,0)^\dagger$ and $\mathbf{e}_{j,-1} = (0,1)^\dagger$, $j = 1, \cdots, b$, then $\mathbf{e}_{j,\pm 1}$ are eigenvectors of Pauli matrix $\boldsymbol{\sigma}_j^z$ corresponding to eigenvalues ± 1. For the classical Ising model, given a configuration $\mathbf{s} = (s_1, \cdots, s_b)$ with energy $\mathbf{H}_I^c(\mathbf{s})$ in (3.2), we define a unit vector in $\mathbb{C}^d$ as follows, $\mathbf{e}_{\mathbf{s}} = \mathbf{e}_{1,s_1} \otimes \mathbf{e}_{2,s_2} \cdots \otimes \mathbf{e}_{b,s_b}$. We show that $\mathbf{e}_{\mathbf{s}}$ is an eigenvector of $\mathbf{H}_I^q$ with corresponding eigenvalue $\mathbf{H}_I^c(\mathbf{s})$. Indeed,

$$
\begin{aligned}
&\boldsymbol{\sigma}_j^z \mathbf{e}_{j,s_j} = s_j \mathbf{e}_{j,s_j},\\
&\left(\mathbf{I}_2 \otimes \cdots \mathbf{I}_2 \otimes \boldsymbol{\sigma}_j^z \otimes \mathbf{I}_2 \cdots \otimes \mathbf{I}_2\right)\left(\mathbf{e}_{1,s_1} \otimes \mathbf{e}_{2,s_2} \cdots \otimes \mathbf{e}_{b,s_b}\right) = s_j \mathbf{e}_{1,s_1} \otimes \mathbf{e}_{2,s_2} \cdots \otimes \mathbf{e}_{b,s_b} = s_j \mathbf{e}_{\mathbf{s}},\\
&\left(\mathbf{I}_2 \otimes \cdots \mathbf{I}_2 \otimes \boldsymbol{\sigma}_i^z \otimes \mathbf{I}_2 \cdots \mathbf{I}_2 \otimes \boldsymbol{\sigma}_j^z \otimes \mathbf{I}_2 \cdots \otimes \mathbf{I}_2\right) = s_i s_j \mathbf{e}_{1,s_1} \otimes \mathbf{e}_{2,s_2} \cdots \otimes \mathbf{e}_{b,s_b} = s_i s_j \mathbf{e}_{\mathbf{s}},
\end{aligned}
$$

it follows that

$$
\begin{aligned}
\mathbf{H}_I^q \mathbf{e}_{\mathbf{s}} = \quad & - \sum_{(i,j)\in\mathcal{E}(\mathcal{G})} J_{ij} \left(\mathbf{I}_2 \otimes \cdots \mathbf{I}_2 \otimes \boldsymbol{\sigma}_i^z \otimes \mathbf{I}_2 \cdots \mathbf{I}_2 \otimes \boldsymbol{\sigma}_j^z \otimes \mathbf{I}_2 \cdots \otimes \mathbf{I}_2\right)\left(\mathbf{e}_{1,s_1} \otimes \mathbf{e}_{2,s_2} \cdots \otimes \mathbf{e}_{b,s_b}\right)\\
& - \sum_{j\in\mathcal{V}(\mathcal{G})} h_j \left(\mathbf{I}_2 \otimes \cdots \mathbf{I}_2 \otimes \boldsymbol{\sigma}_j^z \otimes \mathbf{I}_2 \cdots \otimes \mathbf{I}_2\right)\left(\mathbf{e}_{1,s_1} \otimes \mathbf{e}_{2,s_2} \cdots \otimes \mathbf{e}_{b,s_b}\right)\\
= \quad & - \sum_{(i,j)\in\mathcal{E}(\mathcal{G})} J_{ij} s_i s_j \mathbf{e}_{\mathbf{s}} - \sum_{j\in\mathcal{V}(\mathcal{G})} h_j s_j \mathbf{e}_{\mathbf{s}}\\
= \quad & \left[- \sum_{(i,j)\in\mathcal{E}(\mathcal{G})} J_{ij} s_i s_j - \sum_{j\in\mathcal{V}(\mathcal{G})} h_j s_j\right] \mathbf{e}_{\mathbf{s}}\\
= \quad & \mathbf{H}_I^c(\mathbf{s}) \mathbf{e}_{\mathbf{s}}.
\end{aligned}
$$

Thus, the 2^b eigenvalues of $\mathbf{H}_I^q$ are $\mathbf{H}_I^c(\mathbf{s})$, $\mathbf{s} \in \{+1, -1\}^b$, which are actually the diagonal entries of $\mathbf{H}_I^q$. If $\mathbf{s}_0$ achieves the global minimum of $\mathbf{H}_I^c(\mathbf{s})$, then $\mathbf{H}_I^c(\mathbf{s}_0)$ is the smallest eigenvalue of $\mathbf{H}_I^q$.

The partition function and Gibbs state of the quantum Ising model are, respectively, given by

$$
Z = \mathrm{tr}[e^{-\beta \mathbf{H}_I^q}], \qquad \boldsymbol{\rho} = \frac{e^{-\beta \mathbf{H}_I^q}}{Z}.
$$

Since $\mathbf{H}_I^q$ has eigenvalues $\mathbf{H}_I^c(\mathbf{s})$ with eigenvectors $\mathbf{e}_{\mathbf{s}}$, it is easy to compute the partition function as follows,

$$
Z = \sum_{\mathbf{s}} \langle \mathbf{e}_{\mathbf{s}} | e^{-\beta \mathbf{H}_I^q} | \mathbf{e}_{\mathbf{s}} \rangle = \sum_{\mathbf{s}} e^{-\beta \mathbf{H}_I^c(\mathbf{s})},
$$

The probability of observing configuration $\mathbf{s}$ is given by

$$\langle \mathbf{e_s}|\boldsymbol{\rho}|\mathbf{e_s}\rangle = \frac{1}{Z}\langle \mathbf{e_s}|e^{-\beta \mathbf{H}_I^q}|\mathbf{e_s}\rangle = \frac{1}{Z}e^{-\beta \mathbf{H}_I^c(\mathbf{s})},$$

which is equal to the classical Boltzmann distribution.

6.2 Proof of Theorem 3

Let $u = t/t_f$ be the dimensionless time, and set

$$\mathbf{H}(u) \equiv \mathbf{H}_{QA}(u\, t_f) = \mathbf{H}_{QA}(t), \qquad |\varphi(u)\rangle \equiv |\psi(u\, t_f)\rangle = |\psi(t)\rangle.$$

Since state $|\psi(t)\rangle$of the quantum system in nature time t follows the Schrödingier equation (2.1) with Hamiltonian $\mathbf{H}_{QA}(t)$, $|\varphi(u)\rangle$ satisfies

$$i\frac{d|\varphi(u)\rangle}{du} = t_f \mathbf{H}(u)|\varphi(u)\rangle, \tag{6.10}$$

where we reserve i for the unit imaginary number $\sqrt{-1}$ in the proof of Theorem 3.

Since our goal is to study how close the quantum state is to the ground state, we naturally express the quantum state by the instantaneous eigenstates of $\mathbf{H}(u)$. Let $\lambda_0(u) < \lambda_1(u) < \cdots < \lambda_k(u) < \cdots$ be the eigenvalues of $\mathbf{H}(u)$ listed in an increasing order, and denote by $|k^{(\ell)}(u)\rangle$ the normalized instantaneous eigenstates of $\mathbf{H}(u)$ corresponding to the k-th eigenvalue $\lambda_k(u)$. For example, there are ζ ground states $|0^{(\ell)}(u)\rangle$, $\ell = 1, \cdots, \zeta$, corresponding to the smallest eigenvalue $\lambda_0(u)$. Since our main analysis is targeted for the ground states, we focus on $|0^{(\ell)}(u)\rangle$, their amplitudes and relationships with other eigenstates.

First we need to adjust the eigenstates to meet certain conditions in order to facilitate our analysis. From $\mathbf{H}(u)|j^{(l)}(u)\rangle = \lambda_j(u)|j^{(l)}(u)\rangle$, we take derivatives on both sides to obtain

$$\frac{d\mathbf{H}(u)}{du}|j^{(l)}(u)\rangle + \mathbf{H}(u)\frac{d|j^{(l)}(u)\rangle}{du} = \frac{d\lambda_j(u)}{du}|j^{(l)}(u)\rangle + \lambda_j(u)\frac{d|j^{(l)}(u)\rangle}{du},$$

and thus for $k \neq j$,

$$\begin{aligned} & \langle k^{(\ell)}(u)|\frac{d\mathbf{H}(u)}{du}|j^{(l)}(u)\rangle + \langle k^{(\ell)}(u)|\mathbf{H}(u)\frac{d|j^{(l)}(u)\rangle}{du} \\ = \;& \langle k^{(\ell)}(u)|\frac{d\lambda_j(u)}{du}|j^{(l)}(u)\rangle + \langle k^{(\ell)}(u)|\lambda_j(u)\frac{d|j^{(l)}(u)\rangle}{du}. \end{aligned} \tag{6.11}$$

For orthonormal $|j^{(l)}(u)\rangle$ and $|k^{(\ell)}(u)\rangle$, $\langle j^{(l)}(u)\rangle|k^{(\ell)}(u)\rangle = 0$ and $\langle k^{(\ell)}(u)|\mathbf{H}(u) = \lambda_k(u)\langle k^{(\ell)}(u)|$. Substitute these into (6.11) to yield

$$\begin{aligned} & \langle k^{(\ell)}(u)|\frac{d\mathbf{H}(u)}{du}|j^{(l)}(u)\rangle + \lambda_k(u)\langle k^{(\ell)}(u)|\frac{d|j^{(l)}(u)\rangle}{du} \\ = \;& \frac{d\lambda_j(u)}{du}\langle k^{(\ell)}(u)|j^{(l)}(u)\rangle + \lambda_j(u)\langle k^{(\ell)}(u)|\frac{d|j^{(l)}(u)\rangle}{du} \\ = \;& \lambda_j(u)\langle k^{(\ell)}(u)|\frac{d|j^{(l)}(u)\rangle}{du}, \end{aligned}$$

which leads to

$$\langle k^{(\ell)}(u)|\frac{d}{du}|j^{(l)}(u)\rangle \equiv \langle k^{(\ell)}(u)|\frac{d|j^{(l)}(u)\rangle}{du} = \frac{1}{\lambda_j(u)-\lambda_k(u)}\langle k^{(\ell)}(u)|\frac{d\mathbf{H}(u)}{du}|j^{(l)}(u)\rangle, \quad (6.12)$$

for $j \neq k$. Let $|\check{j}^{(l)}(u)\rangle = \exp\{i\eta_j^{(l)}(u)\}|j^{(l)}(u)\rangle$ be a time-dependent phase shift of $|j^{(l)}(u)\rangle$, that is, we add an accent mark $\check{}$ to mean a time-dependent shift for the eigenstates, where $\eta_j^{(l)}(u)$ satisfies

$$\langle j^{(l)}(u)|\frac{d}{du}|j^{(l)}(u)\rangle + i\frac{d\eta_j^{(l)}(u)}{du} = 0,$$

which is possible since

$$\langle j^{(l)}(u)|\frac{d}{du}|j^{(l)}(u)\rangle + \left(\langle j^{(l)}(u)|\frac{d}{du}|j^{(l)}(u)\rangle\right)^\dagger = \frac{d}{du}\langle j^{(l)}(u)|j^{(l)}(u)\rangle = 0,$$

and hence $\langle j^{(l)}(u)|\frac{d}{du}|j^{(l)}(u)\rangle$ is a pure imaginary number. Thus,

$$\begin{aligned}
&\langle \check{j}^{(l)}(u)|\frac{d}{du}|\check{j}^{(l)}(u)\rangle = e^{i\eta_j^{(l)}(u)}\langle \check{j}^{(l)}(u)|\frac{d}{du}|j^{(l)}(u)\rangle + i\frac{d\eta_j^{(l)}(u)}{du}\langle \check{j}^{(l)}(u)|\check{j}^{(l)}(u)\rangle \\
= \;& e^{i\eta_j^{(l)}(u)}e^{-i\eta_j^{(l)}(u)}\langle j^{(l)}(u)|\frac{d}{du}|j^{(l)}(u)\rangle + i\frac{d\eta_j^{(l)}(u)}{du} \\
= \;& \langle j^{(l)}(u)|\frac{d}{du}|j^{(l)}(u)\rangle + i\frac{d\eta_j^{(l)}(u)}{du} = 0. \quad (6.13)
\end{aligned}$$

Of course $\{|\check{j}^{(l)}(u)\rangle, j = 0, 1, \cdots, \}$ remains to be orthonormal, the pair $(\lambda_j(u), |\check{j}^{(l)}(u)\rangle)$ still satisfies

$$\mathbf{H}(u)|\check{j}^{(l)}(u)\rangle = e^{i\eta_j^{(l)}(u)}\mathbf{H}(u)|j^{(l)}(u)\rangle = e^{i\eta_j^{(l)}(u)}\lambda_j(u)|j^{(l)}(u)\rangle = \lambda_j(u)|\check{j}^{(l)}(u)\rangle,$$

and for $j \neq k$,

$$\begin{aligned}
&\langle \check{k}^{(\ell)}(u)|\frac{d}{du}|\check{j}^{(l)}(u)\rangle = e^{i\eta_j^{(l)}(u)}\langle \check{k}^{(\ell)}(u)|\frac{d}{du}|j^{(l)}(u)\rangle + i\frac{d\eta_j^{(l)}(u)}{du}\langle \check{k}^{(\ell)}(u)|\check{j}^{(l)}(u)\rangle \\
= \;& e^{i[\eta_j^{(l)}(u)-\eta_k^{(\ell)}(u)]}\langle k^{(\ell)}(u)|\frac{d}{du}|j^{(l)}(u)\rangle \\
= \;& \frac{e^{i[\eta_j^{(l)}(u)-\eta_k^{(\ell)}(u)]}}{\lambda_j(u)-\lambda_k(u)}\langle k^{(\ell)}(u)|\frac{d\mathbf{H}(u)}{du}|j^{(l)}(u)\rangle \\
= \;& \frac{1}{\lambda_j(u)-\lambda_k(u)}\langle \check{k}^{(\ell)}(u)|\frac{d\mathbf{H}(u)}{du}|\check{j}^{(l)}(u)\rangle, \quad (6.14)
\end{aligned}$$

where the third equality is due to (6.12).

Now with (6.13)-(6.14) satisfied by the instantaneous eigenstates $\check{j}^{(l)}(u)$ of $\mathbf{H}(u)$, we use them to express the quantum state $|\varphi(u)\rangle$ as follows,

$$|\varphi(u)\rangle = \sum_{j,l\geq 0}\alpha_j^{(l)}(u)|\check{j}^{(l)}(u)\rangle. \quad (6.15)$$

Plugging above expression into the Schrödinger equation (6.10) we obtain

$$\sum_{j,l\geq 0} i\frac{d}{du}\left[\alpha_j^{(l)}(u)|\check{j}^{(l)}(u)\rangle\right] = \sum_{j,l\geq 0} t_f \mathbf{H}(u)\left[\alpha_j^{(l)}(u)|\check{j}^{(l)}(u)\rangle\right],$$

and simple manipulations lead to

$$\begin{aligned}
&\sum_{j,l\geq 0} i\left[\frac{d\alpha_j^{(l)}(u)}{du}|\check{j}^{(l)}(u)\rangle + \alpha_j^{(l)}(u)\frac{d}{du}|\check{j}^{(l)}(u)\rangle\right] = \sum_{j,l\geq 0} t_f \alpha_j^{(l)}(u)\mathbf{H}(u)|\check{j}^{(l)}(u)\rangle \\
= &\sum_{j,l\geq 0} t_f \alpha_j^{(l)}(u)\lambda_j(u)|\check{j}^{(l)}(u)\rangle.
\end{aligned}$$

Taking products with state $\langle\check{k}^{(\ell)}(u)|$ on both sides and noting the scalar nature of t_f, $\alpha_j^{(l)}(u)$ and $\lambda_j(u)$, we arrive at

$$\begin{aligned}
&\sum_{j,l\geq 0} i\left[\frac{d\alpha_j^{(l)}(u)}{du}\langle\check{k}^{(\ell)}(u)|\check{j}^{(l)}(u)\rangle + \alpha_j^{(l)}(u)\langle\check{k}^{(\ell)}(u)|\frac{d}{du}|\check{j}^{(l)}(u)\rangle\right] \\
= &\sum_{j,l\geq 0} t_f \lambda_j(u)\alpha_j^{(l)}(u)\langle\check{k}^{(\ell)}(u)|\check{j}^{(l)}(u)\rangle,
\end{aligned}$$

which can be simplified by (6.13) and the orthonormality of $|\check{j}^{(l)}(u)\rangle$ as

$$\begin{aligned}
&\frac{d\alpha_k^{(\ell)}(u)}{du} + \sum_{l\neq\ell}\alpha_k^{(l)}\langle\check{k}^{(\ell)}(u)|\frac{d}{du}|\check{k}^{(l)}(u)\rangle + \sum_{j\neq k}\sum_l \alpha_j^{(l)}(u)\langle\check{k}^{(\ell)}(u)|\frac{d}{du}|\check{j}^{(l)}(u)\rangle \\
= &-it_f\lambda_k(u)\alpha_k^{(\ell)}(u). \qquad (6.16)
\end{aligned}$$

Use (6.14) to re-write (6.16) with $k = 0$ as a linear differential equation system for the amplitudes $\alpha_0^{(\ell)}(u)$ of ζ ground states

$$\begin{aligned}
\frac{d\alpha_0^{(\ell)}(u)}{du} &= -it_f\lambda_0(u)\alpha_0^{(\ell)}(u) - \sum_{l\neq\ell}\alpha_0^{(l)}(u)\langle\check{0}^{(\ell)}(u)|\frac{d}{du}|\check{0}^{(l)}(u)\rangle \\
&\quad - \sum_{j>0}\sum_l \alpha_j^{(l)}(u)\frac{1}{\lambda_j(u)-\lambda_0(u)}\langle\check{0}^{(\ell)}(u)|\frac{d\mathbf{H}(u)}{du}|\check{j}^{(l)}(u)\rangle, \qquad (6.17)
\end{aligned}$$

where $\ell = 1, \cdots, \zeta$, the sum in the second term is $l = 1, \ldots, \ell-1, \ell+1, \ldots, \zeta$ for ground states, and the sums in the third term are over for all excited states.

The linear differential equation system (6.17) has solution

$$\begin{aligned}
(\alpha_0^{(1)}(u), \cdots, \alpha_0^{(\zeta)}(u))' &= \mathbf{U}(u)(\alpha_0^{(1)}(0), \cdots, \alpha_0^{(\zeta)}(0))' \\
&+ \mathbf{U}(u)\int_0^u [\mathbf{U}(x)]^{-1}\sum_{j>0}\alpha_j^{(l)}(x)\frac{1}{\lambda_j(x)-\lambda_0(x)}\langle\check{\mathbf{0}}(x)|\frac{d\mathbf{H}(x)}{dx}|\check{j}^{(l)}(x)\rangle dx, \qquad (6.18)
\end{aligned}$$

where $\langle\check{\mathbf{0}}(x)| = (\langle\check{0}^{(1)(x)}|, \cdots, \langle\check{0}^{(\zeta)}(x)|)'$, and $\mathbf{U}$ is a fundamental matrix for the homogeneous linear differential equation system corresponding to (6.17) with initial condition $\mathbf{U}(0) = \mathbf{I}$, that is, the columns of $\mathbf{U}$ form a complete linearly independent set of solutions for the homogeneous equation system,

$$\frac{d\alpha_0^{(\ell)}(u)}{du} = -it_f\lambda_0(u)\alpha_0^{(\ell)}(u) - \sum_{l\neq\ell}\langle\check{0}^{(\ell)}(u)|\frac{d}{du}|\check{0}^{(l)}(u)\rangle\,\alpha_0^{(l)}(u),$$

or in a vector-matrix form

$$\frac{d(\alpha_0^{(1)}(u), \cdots, \alpha_0^{(\zeta)}(u))'}{du} = \mathbf{D}(u)(\alpha_0^{(1)}(0), \cdots, \alpha_0^{(\zeta)}(0))',$$

where $\mathbf{D}(u) = -it_f\lambda_0(u)\mathbf{I} - i\mathbf{A}(u)$ is a matrix of size ζ, where $\mathbf{A}(u) = (A_{\ell l}(u))$ and $A_{\ell l}(u) = -i\langle\check{0}^{(\ell)}(u)|\frac{d}{du}|\check{0}^{(l)}(u)\rangle$ for $l \neq \ell$ and 0 for $l = \ell$. Since

$$iA_{\ell l}(u) + [iA_{l\ell}(u)]^* = \langle 0^{(\ell)}(u)|\frac{d}{du}|0^{(l)}(u)\rangle + \left(\langle 0^{(l)}(u)|\frac{d}{du}|0^{(\ell)}(u)\rangle\right)^* = \frac{d}{du}\langle 0^{(\ell)}(u)|0^{(l)}(u)\rangle = 0,$$

$\mathbf{A}(u)$ is a Hermitian matrix. Matrix $\mathbf{U}$ has an expression through the so called Magnus expansion Blanes et al. (2009),

$$\mathbf{U}(u) = \exp\{-it_f\lambda_0(u)\mathbf{I} - \mathbf{\Xi}(u)\}, \quad \mathbf{\Xi}(u) = \sum_{k=1}^{\infty} i^k\mathbf{\Xi}_k(u),$$

where $\mathbf{\Xi}_k(u)$ in the Magnus expansion can be computed by a recursive procedure through the matrices $\mathbf{\Upsilon}_k^{(j)}$ as follows,

$$\mathbf{\Xi}_1(u) = \int_0^u \mathbf{A}(v)dv, \quad \mathbf{\Xi}_k(u) = \sum_{l=1}^{k-1}\frac{B_j}{j}\int_0^u \mathbf{\Upsilon}_k^{(l)}(v)dv, \quad k \geq 2,$$

B_j are Bernoulli numbers,

$$\begin{aligned}
&\mathbf{\Upsilon}_k^{(1)} = [\mathbf{\Xi}_{k-1}, \mathbf{A}], \quad \mathbf{\Upsilon}_k^{(k-1)} = ad_{\mathbf{\Xi}_1}^{(k-1)}(\mathbf{A}),\\
&\mathbf{\Upsilon}_k^{(j)} = \sum_{l=1}^{k-j}[\mathbf{\Xi}_l, \mathbf{\Upsilon}_{k-l}^{(j-1)}], \quad j = 2, \ldots, k-1,\\
&ad_{\mathbf{\Xi}}^0(\mathbf{A}) = \mathbf{A}, \quad ad_{\mathbf{\Xi}}^{k+1}(\mathbf{A}) = [\mathbf{\Xi}, ad_{\mathbf{\Xi}}^k(\mathbf{A})],
\end{aligned}$$

$[\mathbf{A}, \mathbf{B}] = \mathbf{AB} - \mathbf{BA}$ is the matrix commutator of $\mathbf{A}$ and $\mathbf{B}$, $ad_{\mathbf{\Xi}}^k$ is a shorthand for an iterated commutator, and

$$\|\mathbf{\Xi}_k(u)\| \leq \pi\left(\frac{1}{\pi}\int_0^u \|\mathbf{A}(v)\|dv\right)^k.$$

Then

$$\|\mathbf{\Xi}(u)\| \leq \sum_{k=1}^{\infty} \|\mathbf{\Xi}_k(u)\| \leq \pi \sum_{k=1}^{\infty} \left(\frac{1}{\pi}\int_0^u \|\mathbf{A}(v)\|dv\right)^k \leq \int_0^u \|\mathbf{A}(v)\|dv \left(1-\frac{1}{\pi}\int_0^u \|\mathbf{A}(v)\|dv\right)^{-1}$$
$$\leq \int_0^1 \|\mathbf{A}(v)\|dv \left(1-\frac{1}{\pi}\int_0^1 \|\mathbf{A}(v)\|dv\right)^{-1} = \xi,$$

$$e^{-\xi} \leq \exp(-\|\mathbf{\Xi}(u)\|) \leq \|\mathbf{U}(u)\| \leq \exp(\|\mathbf{\Xi}(u)\|) \leq e^{\xi}. \tag{6.19}$$

As the system initializes at the ground states, $\|(\alpha_0^{(1)}(0), \cdots, \alpha_0^{(\zeta)}(0))\|^2 = 1$. From (6.18) and (6.19) we find

$$\|(\alpha_0^{(1)}(1), \cdots, \alpha_0^{(\zeta)}(1))\|_2 \geq \|\mathbf{U}(1)(\alpha_0^{(1)}(0), \cdots, \alpha_0^{(\zeta)}(0))\|^2$$
$$- \left|\mathbf{U}(1)\int_0^1 [\mathbf{U}(x)]^{-1} \sum_{j>0}\sum_{l} \alpha_j^{(l)}(x) \frac{1}{\lambda_j(x)-\lambda_0(x)} \langle \check{\mathbf{0}}(x)| \frac{d\mathbf{H}(x)}{dx} |\check{j}^{(l)}(x)\rangle dx\right|^2, \tag{6.20}$$

$$\|\mathbf{U}(1)(\alpha_0^{(1)}(0), \cdots, \alpha_0^{(\zeta)}(0))\|^2 \geq e^{-\xi}\|(\alpha_0^{(1)}(0), \cdots, \alpha_0^{(\zeta)}(0))\|^2 = e^{-\xi}, \tag{6.21}$$

and

$$\left\|\mathbf{U}(u)\int_0^u [\mathbf{U}(x)]^{-1} \sum_{j>0}\sum_{l} \alpha_j^{(l)}(x) \frac{1}{\lambda_j(x)-\lambda_0(x)} \langle \check{\mathbf{0}}(x)| \frac{d\mathbf{H}(x)}{dx} |\check{j}^{(l)}(x)\rangle dx\right\|^2$$
$$= \left\|\mathbf{U}(u)[\mathbf{U}(x_*)]^{-1} \sum_{j>0}\sum_{l} \alpha_j^{(l)}(x_*) \frac{1}{\lambda_j(x_*)-\lambda_0(x_*)} \langle \check{\mathbf{0}}(x_*)| \frac{d\mathbf{H}(x_*)}{dx} |\check{j}^{(l)}(x_*)\rangle\right\|^2$$
$$\leq \left\|\mathbf{U}(u)[\mathbf{U}(x_*)]^{-1}\right\| \sum_{\ell=1}^{\zeta} \left|\sum_{j>0}\sum_{l} \alpha_j^{(l)}(x_*) \frac{1}{\lambda_j(x_*)-\lambda_0(x_*)} \langle \check{0}^{(\ell)}(x_*)| \frac{d\mathbf{H}(x_*)}{dx} |\check{j}^{(l)}(x_*)\rangle\right|^2$$
$$\leq \|\mathbf{U}(u)\|\|\mathbf{U}^{-1}(x_*)\| \sum_{\ell=1}^{\zeta} \left|\sum_{j>0}\sum_{l} \alpha_j^{(l)}(x_*) \frac{1}{\lambda_j(x_*)-\lambda_0(x_*)} \langle \check{0}^{(\ell)}(x_*)| \frac{d\mathbf{H}(x_*)}{dx} |\check{j}^{(l)}(x_*)\rangle\right|^2$$
$$\leq e^{2\xi} \sum_{\ell=1}^{\zeta} \left|\sum_{j>0}\sum_{l} \alpha_j^{(l)}(x_*) \frac{1}{\lambda_j(x_*)-\lambda_0(x_*)} \langle \check{0}^{(\ell)}(x_*)| \frac{d\mathbf{H}(x_*)}{dx} |\check{j}^{(l)}(x_*)\rangle\right|^2$$
$$\leq \Pi e^{2\xi}\zeta \left[\sum_{j>0}\sum_{l} |\alpha_j^{(l)}(x_*)|\right]^2$$
$$\leq \Pi e^{2\xi}\zeta 2^b \sum_{j>0}\sum_{l} \left|\alpha_j^{(l)}(x_*)\right|^2$$
$$\leq \Pi e^{2\xi}\zeta 2^b (1-p_0), \tag{6.22}$$

where the first equality is from the mean value theorem and $x_* \in (0,1)$, first and third inequalities are due to the spectral norm and (6.19), respectively, and the last two inequalities

are, respectively, from the Cauchy-Schwartz inequality and the facts that

$$p_0 = \min_{0 \le x \le 1} \sum_{\ell=1}^{\zeta} |\alpha_0^{(\ell)}(x)|^2, \qquad \sum_{j,l} |\alpha_j^{(l)}(x)|^2 = 1.$$

The probability of the quantum annealing process staying in the ground states at the final annealing time is equal to the sum of these modulus squares given by the left hand side of (6.20), and thus (6.20)-(6.22) together imply that the probability has the bound stated in the theorem. For $\zeta = 1$, $\mathbf{A}$ is a scalar equal to zero, and hence $\xi = 0$.

6.3 Proof of Lemma 4

By Corollary 5.4 Morita and Nishimori (2008),

$$\sum_{\mathbf{s}_1} |q^1_{M,\beta}(\mathbf{s_1}, t) - q^1_{M,\beta}(\mathbf{s}_1)| \to 0.$$

We have

$$\begin{aligned} q^1_{M,\beta}(\mathbf{s}_1) &= \sum_{k=2}^{M} \sum_{\mathbf{s_k}} \frac{1}{Z_{M,\beta}} \exp\left(\beta \frac{1}{M} \sum_{k=1}^{M} \sum_{\langle ij \rangle} J_{ij} s_{i,k} s_{j,k}\right) \\ &= \frac{1}{Z_{M,\beta}} \exp\left(\beta \frac{1}{M} \sum_{\langle ij \rangle} J_{ij} s_{i,1} s_{j,1}\right) \sum_{k=2}^{M} \sum_{\mathbf{s_k}} \exp\left(\beta \frac{1}{M} \sum_{k=2}^{M} \sum_{\langle ij \rangle} J_{ij} s_{i,k} s_{j,k}\right) \\ &= \frac{1}{Z_{M,\beta}} \exp\left(\beta \frac{1}{M} \sum_{\langle ij \rangle} J_{ij} s_{i,1} s_{j,1}\right) C^*, \end{aligned}$$

where $C^* = \sum_{k=2}^{M} \sum_{\mathbf{s_k}} \exp\left(\beta \frac{1}{M} \sum_{k=2}^{M} \sum_{\langle ij \rangle} J_{ij} s_{i,k} s_{j,k}\right)$. Since

$$\sum_{\mathbf{s}_1} q^1_{M,\beta}(\mathbf{s}_1) = 1,$$

we have

$$\sum_{\mathbf{s}_1} \exp\left(\beta \frac{1}{M} \sum_{\langle ij \rangle} J_{ij} s_{i,1} s_{j,1}\right) = \frac{Z_{M,\beta}}{C^*},$$

which implies

$$q^1_{M,\beta}(\mathbf{s}_1) = \frac{1}{Z^1_{M,\beta}} \exp\left(\frac{\beta}{M} \sum_{\langle ij \rangle} J_{ij} s_{i,1} s_{j,1}\right), \; Z^1_{M,\beta} = \sum_{\mathbf{s}_1} \exp\left(\frac{\beta}{M} \sum_{\langle ij \rangle} J_{ij} s_{i,1} s_{j,1}\right) = Z_{1,\beta/M}.$$

Therefore, $q^1_{M,\beta}(\mathbf{s_1}, t)$ and $q_{1,\beta/M}(\mathbf{s_1}, t)$ are asymptotically the same as $t \to \infty$.

6.4 Proof of Theorem 5

Let

$$X_M = \frac{1}{\sqrt{M}} \sum_{k=1}^{M} \sum_{\langle ij \rangle} J_{ij} s_{i,k} s_{j,k}$$

where $\mathbf{s}$ is generated by $q_{M,\beta}(\mathbf{s})$. Simple algebra shows

$$\begin{array}{ll} & |P(X_M(t) \le x) - P(X_\infty \le x)| \\ \le & |P(X_M \le x) - P(X_\infty \le x)| + |P(X_M(t) \le x) - P(X_M \le x)| \\ = & (I) + (II). \end{array}$$

Consider (I). We have for any given $\theta \in \mathbb{R}$ and $S = \{-1, 1\}^{bM}$,

$$\begin{aligned} E\left[\exp(\theta X_M)\right] &= \sum_{s \in S} \frac{1}{Z_{M,\beta}} \exp\left((\beta + \sqrt{M}\theta) \frac{1}{M} \sum_{k=1}^{M} \sum_{\langle ij \rangle} J_{ij} s_{i,k} s_{j,k} \right) \\ &= \frac{Z_{M,\beta+\sqrt{M}\theta}}{Z_{M,\beta}} \\ &\to \exp\left(\frac{1}{2}\theta^2 \sum_{\langle ij \rangle} J_{ij}^2 \right) \quad \text{as } M \to \infty, \end{aligned}$$

where the last line is due to (6.23) below. We have

$$\begin{aligned} Z_{M,\beta+\sqrt{M}\theta} &= \sum_{\mathbf{s} \in S} \exp\left(\frac{\beta + \sqrt{M}\theta}{M} \sum_{k=1}^{M} \sum_{\langle ij \rangle} J_{ij} s_{i,k} s_{j,k} \right) \\ &= \prod_{k=1}^{M} \sum_{\mathbf{s}_k} \exp\left(\frac{\beta + \sqrt{M}\theta}{M} \sum_{\langle ij \rangle} J_{ij} s_{i,k} s_{j,k} \right) \\ &= \prod_{k=1}^{M} Z_{\frac{\beta+\sqrt{M}\theta}{M}} \\ &= \left(Z_{\frac{\beta+\sqrt{M}\theta}{M}} \right)^M \\ &= \left[Tr\left(\exp\left(\frac{\beta + \sqrt{M}\theta}{M} \sum_{\langle ij \rangle} J_{ij} \sigma_i^z \sigma_j^z \right) \right) \right]^M \\ &= \left[Tr\left(I + \frac{\beta + \sqrt{M}\theta}{M} \sum_{\langle ij \rangle} J_{ij} \sigma_i^z \sigma_j^z + \frac{M\theta^2}{2M^2} \left(\sum_{\langle ij \rangle} J_{ij} \sigma_i^z \sigma_j^z \right)^2 \right) + o(M^{-1}) \right]^M \\ &= \left[2^b + 2^b \frac{\theta^2}{2M} \sum_{\langle ij \rangle} J_{ij}^2 + o(M^{-1}) \right]^M, \end{aligned}$$

where the last equality is by the facts that $Tr(\sigma_i^z \sigma_j^z) = 0$ and $Tr(\sigma_i^z \sigma_j^z \cdot \sigma_{i'}^z \sigma_{j'}^z) = 0$ for $i \neq i'$ or $j \neq j'$. Similarly,

$$Z_{M,\beta} = \left[2^b + O(M^{-2})\right]^M.$$

Thus

$$\begin{aligned} \frac{Z_{M,\beta+\sqrt{M}\theta}}{Z_{M,\beta}} &= \frac{\left[1 + \frac{\theta^2}{2M}\sum_{\langle ij\rangle} J_{ij}^2 + o(M^{-1})\right]^M}{\left[1 + O(M^{-2})\right]^M} \\ &\to \exp\left(\frac{1}{2}\theta^2 \sum_{\langle ij\rangle} J_{ij}^2\right) \quad \text{as } M \to \infty. \end{aligned} \tag{6.23}$$

By Levy continuity Theorem for the moment generating function (Theorem 7.5 in Kapadia et al. (2005)), we have

$$X_M \xrightarrow{d} X_\infty,$$

where X_∞ follows the normal distribution with mean zero and variance $\sum_{\langle ij\rangle} J_{ij}^2$. Thus there is $M_0(\cdot)$ such that for any $M \geq M_0(\epsilon)$,

$$|P(X_M \leq x) - P(X_\infty \leq x)| \leq \epsilon/2. \tag{6.24}$$

Consider (II). Now we fix $M \geq M_0(\epsilon)$. By Corollary 5.4 in Morita and Nishimori (2008), there is $t_0(\epsilon, M)$ such that for all $t \geq t_0(\epsilon, M)$ and all x,

$$|P(X_M(t) \leq x) - P(X_M \leq x)| \leq \epsilon/2. \tag{6.25}$$

By (6.24) and (6.25), the statement is proved.

6.5 Proof of Lemma 7

Let

$$H_D = \sum_{\langle ij\rangle} J_{ij}\sigma_i^z\sigma_j^z \quad \text{and} \quad H_N = \Gamma(t)\sum_i \sigma_i^x.$$

We have

$$\begin{aligned} Z_\beta(t) &= Tr\left(\exp\left(\beta[H_D + H_N]\right)\right) \\ &= Tr\left(\prod_{k=1}^M \exp\left(\frac{\beta}{M}[H_D + H_N]\right)\right) \\ &= Tr\left(\prod_{k=1}^M \exp\left(\frac{\beta}{M}[H_D + H_N]\right)\left(\sum_{i_k=1}^{2^b} \mathbf{e}_{i_k}\mathbf{e}_{i_k}^T\right)\right) \\ &= Tr\left(\sum_{i_M=1}^{2^b}\cdots\sum_{i_1=1}^{2^b} \exp\left(\frac{\beta}{M}[H_D + H_N]\right)\mathbf{e}_{i_1}\mathbf{e}_{i_1}^T \exp\left(\frac{\beta}{M}[H_D + H_N]\right)\right. \end{aligned}$$

$$
\begin{aligned}
&\times \mathbf{e}_{i_2}\mathbf{e}_{i_2}^T \cdots \mathbf{e}_{i_{M-1}}^T \exp\left(\frac{\beta}{M}[H_D + H_N]\right)\mathbf{e}_{i_M}\mathbf{e}_{i_M}^T\Bigg) \\
= &\sum_{i_M=1}^{2^b} \cdots \sum_{i_1=1}^{2^b} \mathbf{e}_{i_M}^T \exp\left(\frac{\beta}{M}[H_D + H_N]\right)\mathbf{e}_{i_1}\mathbf{e}_{i_1}^T \exp\left(\frac{\beta}{M}[H_D + H_N]\right) \\
&\times \mathbf{e}_{i_2}\mathbf{e}_{i_2}^T \cdots \mathbf{e}_{i_{M-1}}^T \exp\left(\frac{\beta}{M}[H_D + H_N]\right)\mathbf{e}_{i_M}, \qquad (6.26)
\end{aligned}
$$

where $\mathbf{e}_k, k = 1, \ldots, 2^b$, are the canonical basis. Let $\mathbf{e}_k = e_{k,1} \otimes e_{k,2} \otimes \cdots \otimes e_{k,b}$, where $e_{k,i}$ is one of $(1,0)^T$ and $(0,1)^T$. Let $s_{k,i} = 1$ if $e_{k,i} = (1,0)^T$ and $s_{k,i} = -1$ if $e_{k,i} = (0,1)^T$. For any $l, k \in \{1, \ldots, 2^b\}$,

$$
\begin{aligned}
&\mathbf{e}_l^T \exp\left(\frac{\beta}{M}[H_D + H_N]\right)\mathbf{e}_k \\
= \quad &\mathbf{e}_l^T \exp\left(\frac{\beta}{M}H_D\right)\exp\left(\frac{\beta}{M}H_N\right)\mathbf{e}_k + \frac{\beta^2}{2M^2}\mathbf{e}_l^T(H_N H_D - H_D H_N)\mathbf{e}_k + O\left((\beta/M)^3\right) \\
= \quad &\exp\left(\frac{\beta}{M}\mathbf{e}_l^T H_D \mathbf{e}_l\right)\mathbf{e}_l^T \exp\left(\frac{\beta}{M}H_N\right)\mathbf{e}_k + O\left((\beta/M)^2\right) \\
= \quad &\left(\sqrt{\frac{1}{2}\sinh\frac{2\beta\Gamma(t)}{M}}\right)^b \exp\left(\frac{\beta}{M}\sum_{\langle ij\rangle} J_{ij}s_{l,i}s_{l,j} + \frac{1}{2}\log\left(\coth\frac{\beta\Gamma(t)}{M}\right)\sum_{i=1}^b s_{l,i}s_{k,i}\right) \\
&+O\left((\beta/M)^2\right), \qquad (6.27)
\end{aligned}
$$

where the second equality is derived using the Taylor expansion, and the last equality is due to (6.28) and (6.29). We have

$$
\mathbf{e}_l^T H_D \mathbf{e}_l = \sum_{\langle ij\rangle} J_{ij}(e_{l,i}^T\sigma^z e_{l,i})(e_{l,j}^T\sigma^z e_{l,j}) = \sum_{\langle ij\rangle} J_{ij}s_{l,i}s_{l,j}. \qquad (6.28)
$$

Since $\sigma_i^x, i = 1, \ldots, b$, commute each other, we have

$$
\begin{aligned}
&\mathbf{e}_l^T \exp\left(\frac{\beta}{M}H_N\right)\mathbf{e}_k \\
&= \mathbf{e}_l^T \prod_{k=1}^b \exp\left(\frac{\beta\Gamma(t)}{M}\sigma_k^x\right)\mathbf{e}_k \\
&= \mathbf{e}_l^T\left[\exp\left(\frac{\beta\Gamma(t)}{M}\sigma^x\right)\otimes\cdots\otimes\exp\left(\frac{\beta\Gamma(t)}{M}\sigma^x\right)\right]\mathbf{e}_k \\
&= \left[e_{l,1}^T \exp\left(\frac{\beta\Gamma(t)}{M}\sigma^x\right)e_{k,1}\otimes\cdots\otimes e_{l,b}^T\exp\left(\frac{\beta\Gamma(t)}{M}\sigma^x\right)e_{k,b}\right] \\
&= \left(\sqrt{\frac{1}{2}\sinh\frac{2\beta\Gamma(t)}{M}}\right)^b \prod_{i=1}^b \exp\left(\frac{1}{2}\log\left(\coth\frac{\beta\Gamma(t)}{M}\right)s_{l,i}s_{k,i}\right) \\
&= \left(\sqrt{\frac{1}{2}\sinh\frac{2\beta\Gamma(t)}{M}}\right)^b \exp\left(\frac{1}{2}\log\left(\coth\frac{\beta\Gamma(t)}{M}\right)\sum_{i=1}^b s_{l,i}s_{k,i}\right) \qquad (6.29)
\end{aligned}
$$

where the second equality is derived by $e^A \otimes e^B = e^{A\oplus B}$ and $(A\otimes B)(C\otimes D) = (AC)\otimes(BD)$, and the fourth equality is due to (6.30) below.

Note: please check the reasoning for the second equality

We have

$$\begin{aligned} & \exp\left(\frac{\beta\Gamma(t)}{M}\sigma^x\right) \\ = & \begin{pmatrix} \cosh\frac{\beta\Gamma(t)}{M} & \sinh\frac{\beta\Gamma(t)}{M} \\ \sinh\frac{\beta\Gamma(t)}{M} & \cosh\frac{\beta\Gamma(t)}{M} \end{pmatrix} \\ = & \sqrt{\frac{1}{2}\sinh\frac{2\beta\Gamma(t)}{M}} \begin{pmatrix} \exp\left(\frac{1}{2}\log\left(\coth\frac{\beta\Gamma(t)}{M}\right)\right) & \exp\left(-\frac{1}{2}\log\left(\coth\frac{\beta\Gamma(t)}{M}\right)\right) \\ \exp\left(-\frac{1}{2}\log\left(\coth\frac{\beta\Gamma(t)}{M}\right)\right) & \exp\left(\frac{1}{2}\log\left(\coth\frac{\beta\Gamma(t)}{M}\right)\right) \end{pmatrix}. \end{aligned} \tag{6.30}$$

By (6.26) and (6.27), we have

$$\begin{aligned} & Z_\beta(t) \\ = & \left(\sqrt{\frac{1}{2}\sinh\frac{2\beta\Gamma(t)}{M}}\right)^{bM} \sum_{\mathbf{s}_M}\cdots\sum_{\mathbf{s}_1} \exp\left(\frac{\beta}{M}\sum_{k=1}^{M}\sum_{\langle ij\rangle} J_{ij}s_{i,k}s_{j,k} + \gamma_\beta(t)\sum_{k=1}^{M}\sum_{i=1}^{b} s_{i,k}s_{i,k+1}\right) \\ & +O(\beta^2/M^2) \\ = & \left(\sqrt{\frac{1}{2}\sinh\frac{2\beta\Gamma(t)}{M}}\right)^{bM} Z_{M,\beta}(t) + O(\beta^2/M^2). \end{aligned}$$

Acknowledgements: The research of Xinyu Song was supported by the Fundamental Research Funds for the Central Universities (2018110128), China Scholarship Coucil (201806485017), and National Natural Science Foundation of China (Grant No. 11871323). The research of Yazhen Wang was supported in part by NSF grants DMS-1528375 and DMS-1707605. The research of Donggyu Kim was supported in part by KAIST Settlement/Research Subsidies for Newly-hired Faculty grant G04170049 and KAIST Basic Research Funds by Faculty (A0601003029).

References

Aharonov, D. and Ta-Shma, A. (2003). Adiabatic quantum state generation and statistical zero knowledge. In *Proceedings of the thirty-fifth annual ACM symposium on Theory of computing*, pages 20–29. ACM.

Aharonov, D., Van Dam, W., Kempe, J., Landau, Z., Lloyd, S., and Regev, O. (2008). Adiabatic quantum computation is equivalent to standard quantum computation. *SIAM review*, 50(4):755–787.

Albash, T. and Lidar, D. A. (2016). Adiabatic quantum computing. *arXiv preprint arXiv:1611.04471*.

Albash, T., Rønnow, T. F., Troyer, M., and Lidar, D. A. (2015). Reexamining classical and quantum models for the d-wave one processor. *The European Physical Journal Special Topics*, 224(1):111–129.

Bertsimas, D. and Tsitsiklis, J. (1993). Simulated annealing. *Statistical science*, 8(1):10–15.

Bian, Z., Chudak, F., Macready, W. G., Clark, L., and Gaitan, F. (2013). Experimental determination of ramsey numbers. *Physical review letters*, 111(13):130505.

Blanes, S., Casas, F., Oteo, J., and Ros, J. (2009). The magnus expansion and some of its applications. *Physics reports*, 470(5-6):151–238.

Boixo, S., Isakov, S. V., Smelyanskiy, V. N., Babbush, R., Ding, N., Jiang, Z., Bremner, M. J., Martinis, J. M., and Neven, H. (2018). Characterizing quantum supremacy in near-term devices. *Nature Physics*, 14(6):595.

Boixo, S., Smelyanskiy, V. N., Shabani, A., Isakov, S. V., Dykman, M., Denchev, V. S., Amin, M., Smirnov, A., Mohseni, M., and Neven, H. (2014). Computational role of collective tunneling in a quantum annealer. *arXiv preprint arXiv:1411.4036*.

Boixo, S., Smelyanskiy, V. N., Shabani, A., Isakov, S. V., Dykman, M., Denchev, V. S., Amin, M. H., Smirnov, A. Y., Mohseni, M., and Neven, H. (2016). Computational multiqubit tunnelling in programmable quantum annealers. *Nature communications*, 7:10327.

Born, M. and Fock, V. (1928). Beweis des adiabatensatzes. *Zeitschrift für Physik*, 51(3-4):165–180.

Brady, L. T. and van Dam, W. (2016). Quantum Monte Carlo simulations of tunneling in quantum adiabatic optimization. *Physical Review A*, 93(3):032304.

Britton, J. W., Sawyer, B. C., Keith, A. C., Wang, C.-C. J., Freericks, J. K., Uys, H., Biercuk, M. J., and Bollinger, J. J. (2012). Engineered two-dimensional ising interactions in a trapped-ion quantum simulator with hundreds of spins. *Nature*, 484(7395):489.

Brooke, J., Bitko, D., and Aeppli, G. (1999). Quantum annealing of a disordered magnet. *Science*, 284(5415):779–781.

Browne, D. (2014). Quantum computation: Model versus machine. *Nature Physics*, 10(3):179.

Brumfiel, G. (2012). Simulation: Quantum leaps. *Nature News*, 491(7424):322.

Cai, T., Kim, D., Wang, Y., Yuan, M., and Zhou, H. H. (2016). Optimal large-scale quantum state tomography with pauli measurements. *The Annals of Statistics*, 44(2):682–712.

Deutsch, D. (1985). Quantum theory, the church–turing principle and the universal quantum computer. *Proc. R. Soc. Lond. A*, 400(1818):97–117.

DiVincenzo, D. P. (1995). Quantum computation. *Science*, 270(5234):255–261.

Farhi, E., Goldstone, J., and Gutmann, S. (2002). Quantum adiabatic evolution algorithms versus simulated annealing. *arXiv preprint quant-ph/0201031*.

Farhi, E., Goldstone, J., Gutmann, S., Lapan, J., Lundgren, A., and Preda, D. (2001). A quantum adiabatic evolution algorithm applied to random instances of an np-complete problem. *Science*, 292(5516):472–475.

Farhi, E., Goldstone, J., Gutmann, S., and Sipser, M. (2000). Quantum computation by adiabatic evolution. *arXiv preprint quant-ph/0001106*.

Geman, S. and Geman, D. (1984). Stochastic relaxation, gibbs distributions, and the bayesian restoration of images. *IEEE Transactions on pattern analysis and machine intelligence*, (6):721–741.

Hajek, B. (1988). Cooling schedules for optimal annealing. *Mathematics of operations research*, 13(2):311–329.

Holevo, A. S. (2011). *Probabilistic and statistical aspects of quantum theory*, volume 1. Springer Science & Business Media.

Irbäck, A., Peterson, C., and Potthast, F. (1996). Evidence for nonrandom hydrophobicity structures in protein chains. *proceedings of the National Academy of Sciences*, 93(18):9533–9538.

Isakov, S. V., Mazzola, G., Smelyanskiy, V. N., Jiang, Z., Boixo, S., Neven, H., and Troyer, M. (2016). Understanding quantum tunneling through quantum Monte Carlo simulations. *Physical review letters*, 117(18):180402.

Johnson, M. W., Amin, M. H., Gildert, S., Lanting, T., Hamze, F., Dickson, N., Harris, R., Berkley, A. J., Johansson, J., and Bunyk, P. (2011). Quantum annealing with manufactured spins. *Nature*, 473(7346):194.

Jörg, T., Krzakala, F., Kurchan, J., and Maggs, A. C. (2010). Quantum annealing of hard problems. *Progress of Theoretical Physics Supplement*, 184:290–303.

Kadowaki, T. and Nishimori, H. (1998). Quantum annealing in the transverse ising model. *Physical Review E*, 58(5):5355.

Kato, T. (1978). Trotter's product formula for an arbitrary pair of self-adjoint contraction semigroup. *Topics in Func. Anal., Adv. Math. Suppl. Studies*, 3:185–195.

Kirkpatrick, S., Gelatt, C. D., and Vecchi, M. P. (1983). Optimization by simulated annealing. *Science*, 220(4598):671–680.

Majewski, J., Li, H., and Ott, J. (2001). The ising model in physics and statistical genetics. *The American Journal of Human Genetics*, 69(4):853–862.

Martoňák, R., Santoro, G. E., and Tosatti, E. (2002). Quantum annealing by the path-integral Monte Carlo method: The two-dimensional random ising model. *Physical Review B*, 66(9):094203.

McGeoch, C. C. (2014). Adiabatic quantum computation and quantum annealing: Theory and practice. *Synthesis Lectures on Quantum Computing*, 5(2):1–93.

Morita, S. and Nishimori, H. (2008). Mathematical foundation of quantum annealing. *Journal of Mathematical Physics*, 49(12):125210.

Nielsen, M. A. and Chuang, I. L. (2000). *Quantum computation and quantum information*. Cambridge Univ. Press.

O'Gorman, B., Babbush, R., Perdomo-Ortiz, A., Aspuru-Guzik, A., and Smelyanskiy, V. (2015). Bayesian network structure learning using quantum annealing. *The European Physical Journal Special Topics*, 224(1):163–188.

Perdomo-Ortiz, A., Dickson, N., Drew-Brook, M., Rose, G., and Aspuru-Guzik, A. (2012). Finding low-energy conformations of lattice protein models by quantum annealing. *Scientific reports*, 2:571.

Perdomo-Ortiz, A., Fluegemann, J., Narasimhan, S., Biswas, R., and Smelyanskiy, V. N. (2015). A quantum annealing approach for fault detection and diagnosis of graph-based systems. *The European Physical Journal Special Topics*, 224(1):131–148.

Rieffel, E. G., Venturelli, D., O'Gorman, B., Do, M. B., Prystay, E. M., and Smelyanskiy, V. N. (2015). A case study in programming a quantum annealer for hard operational planning problems. *Quantum Information Processing*, 14(1):1–36.

Rieger, H. and Kawashima, N. (1999). Application of a continuous time cluster algorithm to the two-dimensional random quantum ising ferromagnet. *The European Physical Journal B-Condensed Matter and Complex Systems*, 9(2):233–236.

Rønnow, T. F., Wang, Z., Job, J., Boixo, S., Isakov, S. V., Wecker, D., Martinis, J. M., Lidar, D. A., and Troyer, M. (2014). Defining and detecting quantum speedup. *Science*, 345(6195):420–424.

Sakurai, J. and Napolitano, J. (2017). Modern quantum mechanics. *Modern Quantum Mechanics, by JJ Sakurai, Jim Napolitano, Cambridge, UK: Cambridge University Press, 2017*.

Shankar, R. (2012). *Principles of quantum mechanics*. Springer Science & Business Media.

Stauffer, D. (2008). Social applications of two-dimensional ising models. *American Journal of Physics*, 76(4):470–473.

Suzuki, M. (1976). Generalized trotter's formula and systematic approximants of exponential operators and inner derivations with applications to many-body problems. *Communications in Mathematical Physics*, 51(2):183–190.

Trotter, H. F. (1959). On the product of semi-groups of operators. *Proceedings of the American Mathematical Society*, 10(4):545–551.

Wang, Y. (2012). Quantum computation and quantum information. *Statistical Science*, 27(3):373–394.

Wang, Y. (2013). Asymptotic equivalence of quantum state tomography and noisy matrix completion. *The Annals of Statistics*, 41(5):2462–2504.

Wang, Y., Wu, S., and Zou, J. (2016). Quantum annealing with Markov chain Monte Carlo simulations and D-Wave quantum computers. *Statistical Science*, 31(3):362–398.

Wang, Y. and Xu, C. (2015). Density matrix estimation in quantum homodyne tomography. *Statistica Sinica*, pages 953–973.